Master's thesis

NTNU
Norwegian University of Science and Technology
Faculty of Medicine and Health Sciences
Kavli Institute for Systems Neuroscience

Michael Joseph Combs

Investigative anatomical mapping of the *Helicoverpa armigera* antennal lobe via anterograde labeling of olfactory sensory neurons from different antennal sections

Master's thesis in Neuroscience
Supervisor: Elena Ian
Co-supervisor: Bente Gunnveig Berg
May 2022

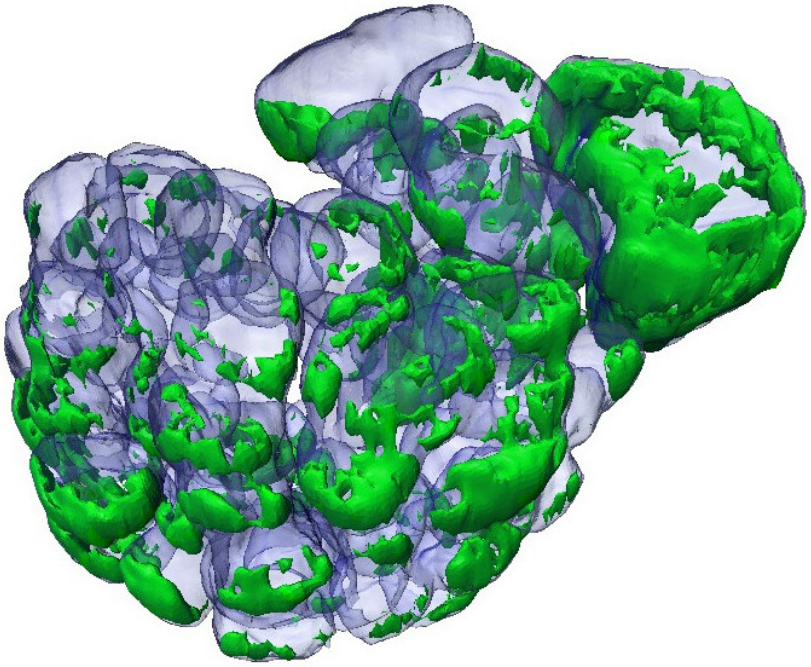

NTNU
Norwegian University of
Science and Technology

Michael Joseph Combs

Investigative anatomical mapping of the *Helicoverpa armigera* antennal lobe via anterograde labeling of olfactory sensory neurons from different antennal sections

Master's thesis in Neuroscience
Supervisor: Elena Ian
Co-supervisor: Bente Gunnveig Berg
May 2022

Norwegian University of Science and Technology
Faculty of Medicine and Health Sciences
Kavli Institute for Systems Neuroscience

NTNU
Norwegian University of
Science and Technology

Preface and Acknowledgements

The work presented here was performed at the Chemosensory Laboratory in the Department of Psychology at the Norwegian University of Science and Technology (NTNU), and the Master's thesis submitted to the Kavli Institute for Systems Neuroscience at the Faculty of Medicine and Health Sciences. In the fulfillment of this work, I have had the privilege of learning a great deal about the nervous system, something for which I am exceedingly grateful. The origins for my journey into neuroscience have their roots in a chance encounter with a girl – as is traditional for the start of many stories, I suppose. After witnessing the suffering brought about by her rare neurological condition, I endeavored to learn as much about the brain as I could, and thus began my study of neuroscience. The knowledge and insights gained during the completion of this entomological body of work, in combination with the roots of my journey, have fully impressed upon me the significance of the minutiae – be they chance encounters, insects, or the everyday actions of one's life. I can only hope that this work contributes a positive effect in whatever small way it may.

I extend my gratitude to my supervisors Elena Ian and Bente Gunnveig Berg for their stewardship; I had much to learn to gain the footing required for the project, and they both were kind and patient enough to teach me what I needed. I would also like to thank fellow lab member Xi Chu for her friendship and for answering my numerous questions. I would not have been able to accomplish this without the help of any of you.

- Michael Joseph Combs

Abstract

The chemosensory system is considered the oldest system from an evolutionary perspective, and it remains well preserved across the animal kingdom. In most organisms, it is split between the two classical senses of taste and smell – gustation and olfaction, respectively. Insects serve as a wonderful model organism for experimental olfactory research, due to both the simplicity of their nervous system as well as how comparable their antennal lobes are to our own olfactory bulb. *Lepidoptera* receive olfactory information primarily through the olfactory sensory neurons situated within the antennae. When the odorants meet the olfactory sensory neurons, various facets of information are transduced into an electrical signal and projected through axons forming the antennal nerves to the primary olfactory center of the insect brain, the antennal lobe, for processing. In this project, the antennal afferent sensory neurons were experimentally bisected at varying lengths and stained with a fluorescent dye. The terminal outputs in the antennal lobe were then scanned with a confocal microscope. Lastly, the data was digitally reconstructed and analyzed. The results confirm previous findings showing that the terminals of the olfactory sensory neurons innervate glomeruli in the ipsilateral antennal lobe. However, the data presented here demonstrate that the sensory neurons innervate the different antennal lobe glomeruli in unequal amounts. This is dependent upon both antennal distance as well as the specific glomerulus in question. In addition, the staining results reveal that a group of medial glomeruli receive very little innervation from the antennal nerve. These results suggest a possible separation of roles between the medial glomeruli from the rest of the ordinary glomeruli. It is unknown currently if the difference in antennal innervation for the medial glomeruli in question is compensated for by an alternate source of innervation. Also of interest was the fact that the largest glomeruli of the macroglomerular complex, the cumulus, was strongly innervated by the sensory neurons along the entire antenna, including those at the periphery.

Sammendrag

Det kjemosensoriske systemet regnes som det eldste systemet fra et evolusjonært perspektiv, og det er godt representert i hele dyreriket. I de fleste organismer består den kjemosensoriske sansen av to systemer – henholdsvis smak og lukt. Insekter fungerer som en velegnet modellorganisme for eksperimentell lukteforskning, både på grunn av det enkle nervesystemet deres, så vel som hvor sammenlignbar deres luktebane er med vår egen – heriblant insektets antennelobe og pattedyrs luktelapp som begge består av glomerulære synaptiske områder. *Lepidoptera* mottar luktinformasjon primært gjennom de luktsensoriske nevronene som er plassert på antennene. Når odorantene bindes til spesifikke reseptorer på disse nevronene, transduseres ulike fasetter av luktinformasjonen til et elektrisk signal som i sin tur projiseres gjennom aksoner som danner antennenerven. Signalet går direkte inn i det primære luktsenteret i insekthjernen, antenneloben. Her ender de sensoriske aksonene i de karakteristiske glomeruli – alle nevroner som uttrykker samme type luktereseptor terminerer i samme glomerulus. I dette prosjektet ble de afferente sensoriske nevronene på antenna farget med et fluorescerende fargestoff fra ulike steder på antenna. Prosjiseringsmønsteret fra disse sensoriske nevronene i antennelobene ble deretter skannet med et konfokalt mikroskop. Til slutt ble dataene rekonstruert og analysert digitalt. Resultatene bekrefter tidligere funn som viser at terminalene til de luktsensoriske nevronene innerverer glomeruli i den ipsilaterale antenneloben. Imidlertid demonstrerer dataene som presenteres her at de sensoriske nevronene innerverer antennelobene ulike glomeruli på en spesifikk måte. Prosjiseringsmønsteret er avhengig av både hvilket nivå på antenna det ble farget fra så vel som den spesifikke glomeruli. I tillegg demonstrerte resultatene at en gruppe mediale glomeruli mottar svært lite innervering fra hele antenna. Disse resultatene antyder at de mediale glomeruli kan inneha en spesifikk roller i forhold til resten av de ordinære glomeruli. Det er foreløpig ukjent om den svake innervasjon for de aktuelle mediale glomeruli blir kompensert for av en alternativ sensorisk kilde. Et annen interessant funn var at det største glomerulus i det hannspesifikke macrogolomerular-komplekset, cumulus, ble bemerkelsesverdig sterkt innervert av sensoriske nevroner langs hele antenna – selv de fra periferien.

Abbreviations

AL: Antennal Lobe

ALT: Antennal Lobe Tract

- dALT: dorsal Antennal Lobe Tract
- dmALT: dorsomedial Antennal Lobe Tract
- lALT: lateral Antennal Lobe Tract
- mALT: medial Antennal Lobe Tract
- mlALT: medio-lateral Antennal Lobe Tract
- tALT: transverse Antennal Lobe Tract

AN: Antennal Nerve

dm-a: anterior dorsomedial unit (relative to cumulus)

dm-p: posterior dorsomedial unit (relative to cumulus)

Fx: Female Complex

GPCR: G Protein-Coupled Receptor

LN: Local interneuron

LPO: Labial Pit Organ

LPOG: Labial Pit Organ Glomerulus

MB: Mushroom Bodies

MGC: Macroglomerular Complex

OB: Olfactory Bulb

OBP: Odorant Binding Protein

ODE: Odorant Degrading Enzyme

OG: Ordinary Glomerulus

OR: Odorant Receptor

OSN: Olfactory Sensory Neuron (previously known as Odorant Receptor Neuron[1])

OSO: Olfactory Sensory Organ

PCx: Posterior Complex

PN: Projection Neuron

PR: Pheromone Receptor

SAP: Sting Aggression Pheromone

[1] ORN and OSN refer to the same item. Ito et al. (2014) established the present hierarchical nomenclature system for insect brains. Previous literature may have utilized the term ORN, but references to those papers will instead utilize OSN to keep terminology internally consistent.

Table of Contents

1. Introduction 01
   1.1. Odorants 01
   1.2. Olfactory sensilla 03
   1.3. Odor receptors 06
   1.4. Primary olfactory processing area 07
   1.5. Secondary olfactory processing area 10
   1.6. Current knowledge and aims of the study 11
2. Materials and methods 12
   2.1. Insect securement 12
   2.2. Insect preparation 12
   2.3. Insect brain dissection and dehydration 13
   2.4. Confocal image acquisition 13
   2.5. Data preparation 14
   2.6. Digital reconstruction and volumetric analysis 14
   2.7. Ethics 15
3. Results 16
   3.1. Innervation patterns from distal cut preparations 16
   3.2. Innervation patterns from medial cut preparations 18
   3.3. Innervation patterns from proximal cut preparations 21
   3.4. General trends and exceptions 23
4. Discussion 27
   4.1. Possible reasons for innervation differences between select glomeruli 27
   4.2. Spatial-temporal encoding of the antennae 29
   4.3. Antennal pheromone reception across all segments 31
   4.4. Possible explanation for lack of medial glomeruli innervation 31
   4.5. OSN pattern similarity present in all AL glomeruli 33
   4.6. Amira selection considerations 33
5. Conclusion 35

References 36

Appendix 43

[1] Introduction

"Chemosensation" is a portmanteau of two terms – "chemo", a linguistic element denoting chemicals – and "sensation", a reaction to external stimulation of the sense organs. The detection of chemical stimuli in the external environment is perhaps the most universal of senses and it remains well preserved across the animal kingdom, to the extent that every animal has it. Even the simplest free living animal, *Trichoplax adhaerens,* an organism that possesses no nerves or sensory cells (Ivanovic & Vlaski-Lafarge, 2016), still utilizes chemosensation (Senatore et al., 2017), underscoring its vital importance to all forms of life. The sensing of chemicals can be broadly categorized into the classical senses of taste and smell – gustation and olfaction, respectively.

Olfaction is the detection of odorants – aromatic molecules suspended in a medium – by the olfactory sensory organs (OSOs), which may ultimately serve as prompts with which to guide behavior. These behaviors may range from finding food; avoiding poisons, toxins, or predators; mate detection and selection; and egg-laying behaviors. Social behaviors are reliant upon olfactory cues as well; honeybees utilize a sting aggression pheromone (SAP) to modulate collective defense, with increasing levels of the SAP increasing collective aggression until a saturation point is reach (Lopez-Incera et al., 2021). The sense of smell is also intricately linked to several physiological and psychological functions: humans who suffer from anosmia also suffer a diminished sense of taste (Kandel et al., 2000); patients with depression have reduced olfactory performance, and patients with olfactory dysfunction have symptoms of depression which worsen with severity of smell loss (Kohli et al., 2016).

It is no understatement to say olfactory information pervades numerous areas of life. As an example, a memory of a night out may include the smells of food; of the night air; the perfume, cologne, soap, or simply body odor of the people if any were present, etc. It is often the case that one lacks the language to describe memory of a smell, but upon reintroduction one will be able to recognize it and often the context within which the smell was associated, due to the associative learning performed in the higher processing areas. The pathway the olfactory input takes from the environment to the periphery of the animal to the higher centers of the brain will be described below.

[1.1] Odorants

Olfactory stimuli are usually termed "odorants", although depending upon context a distinction is often made for signaling molecules from other animals. Odorants are small

volatile molecules, peptides, proteins, and gases such as carbon dioxide or oxygen; some of which can be detected at picomolar concentrations (reviewed by Kaupp, 2010). The molecules used to communicate between animals are known as semiochemicals, the terminology derived from the Greek σημεῖον, transliterated as *semeion* [a mark or signal] (reviewed by Law & Regnier, 1971). The semiochemicals used in interspecies communication can be divided into four categories. Allomones are semiochemicals whose transmission favors the producer, such as those released by plants when being fed upon by insects. Kairomones are semiochemicals whose transmission favors the receiver, an example being the natural aversion that rats display to fox urine (Wernecke et al., 2015). Synomones are the semiochemicals whose detection favor both the emitter and the recipient – when elm leaf beetles prey on field elm leaves, the elm will emit volatiles which attract a species of chalcid wasps which prey on the eggs of the beetle (Meiners & Hilker, 2000). Apneumones are semiochemicals emitted by an abiotic material, which evokes in a second party receiver a favorable behavior or reaction, yet which is detrimental to a third party species that may be found living in or around the abiotic material (Kasinger et al., 2008). Semiochemicals used in intraspecies communication are known as pheromones. These can be utilized in a variety of ways depending upon context, from the SAP emitted by honeybees to the mate-luring pheromones produced by noctuid moths, which will be discussed in further detail later. While the term "odorant" encompasses all odors, the classification of a molecule under "general odorant", "semiochemical", or "pheromone" is contextual: an insect pheromone would be classified as a general odorant for humans.

Detection of odorants is not always sufficient to prompt the appropriate behavior; the concentration and ratio in relation to other odorants are key variables as well. As an example of the concentration being vital, indole is a bacterial product produced by various species such as *Escherichia coli* (Hu et al., 2010) which humans perceive in small concentrations as a somewhat pleasant floral scent; yet in high concentrations it has a repugnant and putrid scent. Whereas an example of the ratio being the determining factor is present in the case of two sympatric species of noctuid moths, *Helicoverpa armigera* and *Helicoverpa assulta*.
The noctuid moths *H. armigera* and *H. assulta* use the same sex pheromones of *cis*-11-hexadecenal (Z11-16:Ald) and *cis*-9-hexadecenal (Z9-16:Ald) in opposing ratios. In *H. armigera* the ratio of (Z9-16:Ald) to (Z11-16:Ald) is 2.1:100 whereas in *H. assulta* the ratio is 1739:100 (Wang et al., 2005). These opposing ratios serve to conserve production and detection architecture while maintaining reproductive isolation – similar findings have been found for other sympatric species of moths such as in the small ermine moth family

Yponomeutidae (Löfstedt et al., 1991). The same molecules in the wrong concentration or ratio will serve as a deterring rather than attracting stimulus.

Context also matters in pheromone communication. Female *H. armigera* use the sex pheromone cis-11-Hexadecenol (Z11-16:OH) in their pheromone blend to indicate an inopportune time to mate; males who were genetically altered to ignore this component of the pheromone blend initiated mating behavior with the immature female anyway, resulting in lower egg viability (Chang et al., 2017). Another example of a context-dependent pheromone would be the male-specific *Drosophila melanogaster* pheromone Z-11-octadecenyl acetate, also known as *cis*-Vaccenyl acetate (cVA), which serves multifunctional uses in *D. melanogaster*. Bartelt et al. (1985) found it to mediate aggregation, and to discourage males from mating with other males as well as recently mated females. This was highlighted in a different way by Kurtovic et al. (2007), who used knock-in models with the odorant receptors (ORs) for cVA replaced with other receptors. They switched out the OR for cVA with an OR for either the yeast transcriptional activator GAL4, the pheromone receptor (PR) associated with the silk moth pheromone bombykol, or the PR for the noctuid *Heliothis virescens* pheromone Z-11:16:Ald. The knock-in models displayed altered behavior from not being able to detect the pheromone from their kin, which was restored upon artificial presentation of the odorant corresponding to the knocked-in OR, showing that rather than detection of the odorant, it is the activation of the OR which prompts behavior, and the odorant is simply a means to the end.

[1.2] Olfactory sensilla

Odorants are detected by olfactory sensory neurons (OSNs) which lay just beneath the cuticle in the organism. While the term “cuticle” in entomology typically refers to the chitin exoskeleton of an insect, the term itself also refers to the outermost epidermal layer of an organism separating – and protecting – them from the environment. The epidermis of human skin would thus be classified accordingly, as an example, as would the waxy outermost layer of leaves and plants which do not possess a periderm. The purpose of the cuticle is to protect the organism and mitigate fluid loss and other contaminants from the environment, but serves an especially important role in their protection for the insect olfactory neurons, as these are not regenerated through adult life without molting (Ando et al., 2019). Thus, the sensilla of insects are covered by a thin, protective cuticular layer in which lay many nanopores which serve to allow odorants to pass through while filtering out other substances (Shields, 2004).

The dendrites of the OSNs reach outwards towards the surface of the cuticle through the OSO, culminating in specialized organelles which house the ORs. For example, in humans, the primary OSO is the olfactory mucosa, containing the supportive lamina propria along with the olfactory epithelium, which is the epithelial tissue responsible for odor reception (reviewed by Suzuki & Osumi, 2015). The olfactory epithelium receives the odorants with cilia, specialized eyelash-like organelles which line the olfactory epithelium inside the roof of the nasal cavity; the Latin *cilium* in fact directly translates to "eyelash". Humans also possess a secondary OSO – the vomeronasal organ, also known as a Jacobson's organ. Postmortem autopsies in humans have revealed the existence of the vomeronasal pit, along with numerous microvillar cells, which are the dominant receptor cells in the vomeronasal organ of all lower vertebrates (Stensaas et al., 1991). The human nose would be considered then a multi-modal sensory structure.

The various sensilla types of insects develop from epithelial sensory organ progenitor cells, putting them on an organizational-level equivalence to organs, and as such would be classified as sensory organs themselves, categorically speaking (Hartenstein, 2005). The individual sensillum would thus be termed organelles, the modern Latin *organella* taken as meaning "[a] little organ" from the old Latin *organum*. The group of "sensilla trichodea" would be an OSO, and each individual sensillum trichodea would be an individual organelle. Like in other insects, in *Lepidoptera* most olfactory stimuli are received through their antennal OSOs. The cuticular structures reminiscent of eyelashes (see Figure 1) act as a filter, allowing odorants to pass through before they eventually contact the dendrites of the bipolar OSNs. While *Lepidoptera* sensilla are primarily located upon their antennae, they also possess these organelles upon the labial palps (Kent et al., 1986), ovipositors (Klinner et al., 2016), feet, and genitals (Hu et al., 2016). The antennae of *Lepidoptera Noctuidae* are multimodal sensory structures which contain not only the olfactory sensilla trichodea, but the thermosensitive and hygrosensitive sensilla styloconica, the mechanosensitive sensilla campaniformia, and the sensilla chaetica which are mechanosensitive as well as possessing gustatory neurons (Zhang et al., 2001).

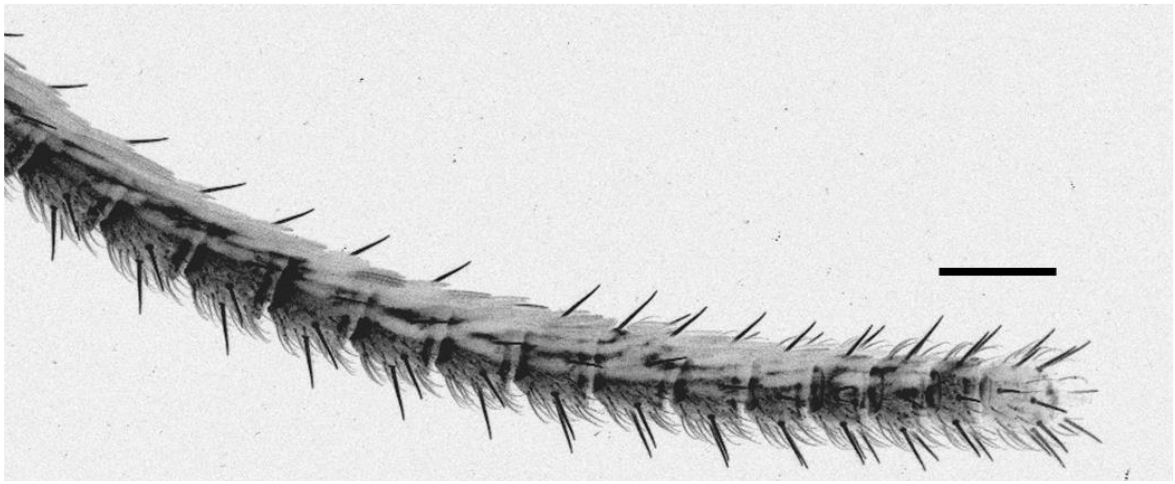

Figure 1: **Confocal image of a female *H. armigera* antenna.**
Sensilla trichodea in grey, sensilla chaetica in black. Scale bar is 100 µm.

Zhang et al. (2001) reported that in noctuid moths, PR cells are found in the long sensilla trichodea which stand out in lateral rows upon the antennae. Mayer et al. (1981) reported that these sensilla trichodea type I in *Trichoplusia ni* comprised 75% of the total antennal sensilla surface area. Single sensillum recordings from noctuid moths of the sub-family *Heliothinae* have demonstrated that every trichodea sensillum contains two to four OSNs which project their axons to the antennal lobe (AL) (Almaas & Mustaparta, 1991); yet despite housing multiple OSNs, no sensilla seems to contain multiple pheromone neurons (Berg et al., 2005). This is likely no mere coincidence, as OSNs have been shown to have their firing responses inhibited by neighboring OSNs (Su et al., 2012). Diongue et al. (2013) found via electron microscopy scanning that although females have more sensilla trichodea than males, the general morphological arrangement and pattern of identified sensory structures were equivalent between the two sexes. These differing types of sensilla were found to be unique in terms of both morphology and location. They further reported that their findings for general morphological patterns of *H. armigera* did not differ from other noctuid moths such as those found for *T.ni* described by Mayer et al. (1981), heavily suggesting a shared taxonomical family similarity. However, these findings differ from those found by Tangtrakulwanich et al. (2011) concerning the sensilla morphology of the stable fly *Stomoxys calcitrans*, solidly establishing an evolutionary divergence of the sensilla. It is thought that this is due to ecological pressures to fulfill certain ecological niches (reviewed by Hallberg & Hansson, 1999; reviewed by Hansson & Stensmyr, 2011).

[1.3] Odorant receptors

Odorant molecules captured by the OSOs are absorbed through the pores upon the surface of the sensilla (Hunger & Steinbrecht, 1998). Odorants do not easily pass through the underlying aqueous sensilla lymph due to the presence of odorant degrading enzymes (ODEs), however when these are bound by the appropriate odorant binding protein (OBP), they become solubilized and escape the effect of the ODEs (Zhang et al., 2015a), enabling them to more easily contact the dendrites of the OSNs. The OBPs are a class of proteins which can be further subdivided into pheromone binding proteins and general odorant-binding proteins. The binding sites of the OBPs in the membrane of the sensilla determine their response to odorant molecules; similarly, the receptor terminal types of the OSN determine the tuning for odorant detection – the OSNs will usually not activate for an incorrect odorant or odorant-OBP complex (Wicher, 2015). Once the OR receives the molecule, it transduces an electric signal in the OSN, and the firing of the action potential is conveyed to the brain.

The sensitivity of the OSNs and ORs can be extremely fine – linked gas chromatography and electrophysiology recordings revealed that some individual OSNs would respond to one or two structurally similar molecules out of hundreds of compounds tested (Rostelien et al., 2000). A neuron response to a single molecule can be responsive to many plant species: the compound linalool is found in over 200 plant species, and represents approximately 70% of the terpenoids of floral scents (Aprotosoaie et al., 2014). OSNs receptive to linalool were found to respond in *H. virescens* and *H. armigera* to headspace volatiles of wild tobacco, sunflower, and several others with little molecular overlap – suggesting that the ORs are tuned to specific odors found in a wide range of host plant species (Rostelien et al., 2005).

Vertebrae ORs are almost exclusively metabotropic, in which the ligand-binding receptors – belonging to the G protein-coupled receptor (GPCR) superfamily – utilize secondary messengers to indirectly activate the ion channels (Silbering & Benton, 2010). Insect ORs, however, utilize ionotropic signaling, which differ from metabotropic signaling in many ways: they possess a different morphology, have a different evolutionary origin, and possess reversed membrane topologies (Benton et al., 2006) of which a visual representation can be seen in Figure 2, showing the insect olfactory receptor as a heteromeric complex of two molecules, the ligand and ligand receptor.

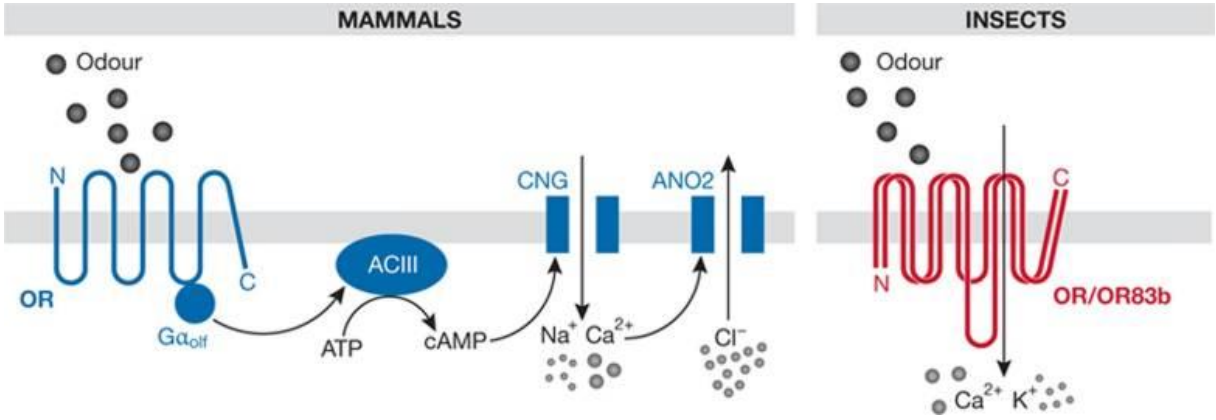

Figure 2: **Comparison of mammalian and insect odorant receptors.**
Schematic of the molecular basis of olfactory signal transduction in the mouse and fruit fly. From Silbering and Benton (2010).

The OR coreceptor, termed Orco (Sato et al., 2008; Vosshall & Hansson, 2011), together with the OR forms a complex serving as both a receptor and an ion channel gated by the binding of the ligand (reviewed by Kaupp, 2010). The dual role of receptor and ion channel gating allows the OR/Orco complex enhanced processing speed, if for no other reason than less steps to go through. The mammalian repertoire of ORs comprises between ~800-1500 members, whereas in insects the number is much smaller. For example, *H. armigera* has 60 (Zhang et al., 2015b), *D. melanogaster* has 62 (Robertson et al., 2003), and the honeybee *Apis mellifera* has 170 (Robertson & Wanner, 2006). The metabotropic signaling and higher number of glomeruli and receptors allow mammals higher discriminatory flexibility and regulation, while the ionotropic signaling and lower number of receptors serves to track rapid changes in olfactory information by the quickly moving airborne insect (reviewed by Kaupp, 2010).

[1.4] Primary olfactory processing area

While vertebrate and insect ORs differ greatly, the basic mechanisms underlying the primary olfactory processing areas are well preserved across species in most phyla, and the insect antennal lobe is analogous to the vertebrae olfactory bulb (OB) (reviewed by Hildebrand & Shepherd, 1997). In insects, the ALs serve as the first stage of the central olfactory pathway and like the OB they possess glomeruli as their characteristic substructures: spheroidal neuropils, separated to different extents by glial processes. Besides being innervated by the OSNs, these glomeruli are innervated by three other cell types – multiglomerular local interneurons (LN), which modulate the olfactory information; centrifugal neurons, which convey top-down information from other brain areas; and

projection neurons (PN), which output olfactory information from the AL into higher brain areas (Kymre et al., 2021). Multiple OSNs of the same type converge in one or two glomeruli in the insect AL in a similar fashion to that of the vertebrate OB (Vosshall et al., 2000). The convergence of these multiple OSNs allow for the averaging, amplification, or inhibition of signals done at the periphery level as a sort of pre-processing before the true primary processing center of the insect brain.

The anatomical organization of the *H. armigera* AL was described by Zhao et al. (2016). The 79 identified glomeruli of *H. armigera* were split into four groups: the sexually dimorphic complexes – the macro glomerular complex (MGC) in males and female complex (Fx) in females, the labial-palp pit organ glomerulus (LPOG) – a carbon dioxide responsive glomerulus, the posterior complex (PCx) – ten glomeruli of unknown specific function forming a specific assembly, and the rest of the 65 glomeruli as ordinary glomeruli (OG).

The MGC serves to help the male insect locate conspecific females and avoid allospecific females through several means. The importance of this processing is reflected in the moth devoting an entire region of the brain solely to serve as a first order relay for pheromones and interspecific signals (Berg et al., 1998). The three glomeruli of the MGC are the cumulus, the dorsomedial anterior unit (dm-a), and the dorsomedial posterior unit (dm-p), with the dm-a and dm-p named in respect to their position relative to the cumulus. In *H. armigera*, the cumulus responds to the primary sexual pheromone component Z11-16:Ald; the dm-a responds to interspecific components Z-9-tetradecenal (Z9-14:Ald) and Z11-16:OH; and the dm-p responds to the secondary pheromones Z9-16:Ald and Z9-14:Ald (Wu et al., 2015). The ratio of Z11-16:Ald to Z9-16:Ald determines whether the signal is processed as an attractant or a deterrent. The molecule Z9-14:Ald is an interspecific constituent produced by other *Noctuidae* species such as *Chloridea virescens* – formerly categorized as *Heliothis virescens* (Pogue, 2013) – it serves as a sexual behavioral antagonist in *H. armigera* (Kehat & Dunkelblum, 1990).

The LPOG is located most ventrally in the AL, anterior to G71-72, and is generally of a larger size than other OG. It is responsible for processing input from OSNs detecting carbon dioxide (CO_2) detection. Higher levels of CO_2 in comparison to ambient levels can indicate imminent danger, overcrowding, and the location of food (Jones, 2013). In *H. armigera* it is predominantly used in conjunction with plant odors for foraging and oviposition behaviors (reviewed by Guerenstein & Hildebrand, 2008). The LPOG receives no innervation from the antennae and is unique in this regard in comparison to the other glomeruli – it receives projections from the labial pit organ (LPO). The innervation of the LPOG is also unique in

that it is the only AL glomerulus which receives bilateral innervation from its primary sensory organ (Kent et al., 1986).

The PCx responds to a variety of stimuli. Frank et al. (2017) found a distinctive region in the PCx of *Drosophila* which represents a simple sensory map with adjacent "hot", "cold", "dry", and "humid" glomeruli. In a previous study on the heliothine species *Helicoverpa zea,* Lee et al. (2006) found one PCx glomerulus receiving input from a male-specific sensory neuron co-located with the neuron tuned to the primary pheromone component.

The OG, including the PCx, are responsible for processing general odorants (reviewd by Mustaparta, 2002). In *H. armigera* these general odorants are predominantly plant odors (Christensen, 2002). The two systems of pheromones to the MGC and general odorants to the ordinary glomeruli are not entirely separated, however, as pheromone reception has been observed in the interneurons within the ordinary glomeruli (Anton & Hansson, 1995).

Within the AL, LNs serve to facilitate inter glomerular communication. Most LNs in insects are GABAergic, and possess diverse morphology – varying in terms of polarity, connectivity, and arborizations (reviewed by Galizia & Rossler, 2010). Many LNs form dendrodendritic synapses with PNs (Kay & Stopfer, 2006). They are responsible for several signal refining processes such as lateral inhibition; synchronization of projection neurons by local oscillatory synchronization; spatial and temporal coding, and the refinement of the aforementioned codes; as well as gain control (reviewed by Laurent, 1999; Seki & Kanzaki, 2008). These processes ultimately improve the signal to noise ratio (Christensen et al., 1993). Among the AL LNs tested, Reisenman et al. (2011) found relatively equal proportions of LNs that display excitatory, inhibitory, and both excitatory and inhibitory responses in proportions of roughly one-third each; they further found that while all the recorded LNs responded to at least one tested odorant, a fifth of them responded to all tested odorants.

The AL PNs connect the AL to the two primary higher olfactory processing areas of the brain – the calyces of the mushroom bodies (MBs) and the lateral horn (LH) – through three main antennal lobe tract (ALT) pathways: the medial ALT (mALT), the mediolateral (mlALT), and the lateral ALT (lALT). These ALTs are primarily formed by axons of the AL PNs correspond to the mammalian olfactory tract targeting regions on the temporal lobe (reviewed by Lledo et al., 2005). Three minor tracts were also identified in moths – the transverse ALT (tALT), the dorsal ALT (dALT), and the dorsomedial ALT (dmALT) (Homberg et al., 1988; Ian et al., 2016b)

Recent entomological research has unveiled more information of the individual PNs within each of these minor tracts (Ian et al., 2016a; Kymre et al., 2021). The major population of neuronal outputs from the AL are uniglomerular PNs, possessing dendritic innervations into a single glomerulus (Anton & Homberg, 1999). The mALT, for example, is formed by uniglomerular PNs projecting to the calyces of the MBs before terminating in the ipsilateral protocerebrum. The mlALT projects to the lateral protocerebrum as well, however they avoid the MB route, and are multiglomerular rather than uniglomerular (Homberg et al., 1988). Lastly the lALT, containing both uniglomerular and multiglomerular neurons, target different protocerebral regions including the column in the superior intermediate protocerebrum, the ventrolateral protocerebrum, the LH, as well as the MB calyces (Ian et al., 2016b). *Noctuidae* have approximately 850 PNs across the six ALTs, although the majority follow the three primary tracts – the mALT, the mlALT, and the lALT (Kymre et al., 2021).

[1.5] Secondary olfactory processing areas

Generally, the MBs and LH serve as the main secondary processing areas of the insect brain for received olfactory information for most species, with exceptions being species like the bristletail *Malachis germanica,* which possess no MBs (reviewed by Galizia & Rossler, 2010).

The MBs receive their innervation in a neuropil region known as the calyx, in which the Kenyon cells of the MBs synapse with the PNs from the AL. The MBs are responsible for associative learning and memory in insects (reviewed by Davis, 1993). Chemical ablation of the mushroom bodies in *Drosophila* removed the capacity for odor learning; flies fed hydroxyurea depleted the cells necessary for the MBs to form, resulting in precise MB ablation with the LH and other parts of the brain left intact (de Belle & Heisenberg, 1994). In all other ways the insects behaved normally but they lacked the capacity for learning derived from classical conditioning. However, the MBs are not solely responsible for associative odor memory formation. In the American cockroach *Periplanta americana* it was found that each PN type innervated a different MB component, providing the means for encoding spatial olfactory information along the neural circuit (Nishino et al., 2018). The MBs also modulate their responses depending on the geometry inlaid in the neural circuit firing patterns. In this way they are also used for spatial decoding of the received olfactory information: distinct sites on the antennae project to distinct areas in the glomeruli, which correspond to specific PNs from the AL.

Along with olfactory information, the LH also receives sensory information from the visual and mechanosensory centers, leading to speculation that it serves to help track odors in flight (Duistermars & Frye, 2010). Intracellular recordings of LH neurons have revealed ten distinct classes of LH neurons, and all of the tested LH neurons responded to every tested odor instead of specific odors for distinct regions or types, suggesting that the LH contributes to concentration coding, bilateral processing, and multimodal integration (Gupta & Stopfer, 2012). Because the LH functions were operating normally when the MB abolition was performed in *Drosophila*, it is believed that the functions of the LH primarily innate, rather than in learning behavior.

[1.6] Current knowledge and aims of the study

One of the most commercially damaging pest species in the world is *H. armigera* (Tay et al., 2013). This polyphagous species causes billions of dollars (US) worth of damages across several countries (reviewed by Haile et al., 2021). The noctuid *H. armigera* detects the odorants and semiochemicals produced by their host plants, as well as the pheromones of noctuid moth species, to an astonishing selectivity and sensitivity (reviewed by Mustaparta, 2002). The females of the species even preferentiate flowering plants for egg-laying sites by their elevated production levels of carbon dioxide (reviewed by Fitt, 1989). The investigation of the *Noctuidae* olfactory system is thus a matter of ongoing interest for study, given the areas of the economic and societal impact of pest control, as well as their importance in serving as a model organism for the human olfactory system.

It is well known that signals concerning general odorants and pheromones are conveyed along different neural pathways from the periphery to the primary olfactory center in *Heliothinae* (reviewed by Berg et al., 2014). However, it is not yet known whether the AL projection patterns originating from different antennal segments differ in *Noctuidae*. This issue is investigated in this master's thesis. With systematic anterograde mass staining of differential flagellum bisection points along the antenna, subsequent confocal scanning of the staining patterns in the AL glomeruli, and the resulting digital reconstructions, this study aims to determine the putative innervation pattern differences across the distinct glomeruli subgroups from the OSNs to further our accumulated body of olfactory knowledge. It is hoped that the results obtained within this body of work will serve as a basis for further research.

[2] Materials and Methods

[2.1] Insect securement

Our chemosensory lab received both male and female *Helicoverpa armigera* pupae from Keyun Biocontrol (Jiyuan, China). The pupae were then separated by their abdominal terminate sex characteristics into sex specific plexiglass containers and kept in climate-controlled chambers (IPP260, Memmert GmbH + Co.KG, Schwabach, Germany) at 24 ºC, 60 % air humidity, and light hours 18:00-08:00 until eclosure. Individuals of similar eclosure times were moved to dated sex specific separate cylindrical plexiglass containers (18 cm x 10 cm) to allow more spacious conditions to lessen stress while ensuring accurate age information. They were provided cellulose sheets for comfort, *ad libitum* access to 10% sucrose solution for nourishment, and returned to the climate chamber until required for experimentation.

[2.2] Insect preparation

A total of 55 insects were utilized to perform 53 experiments. The subjects were gently placed in a small plastic tube to limit movement, with an application of utility wax (Kerr Corporation, Michigan, USA) around the head and neck to further curtail movement. Insect preparations and dissection were performed under a 40x stereo microscope (Leica M60). The antennae were measured with digital calipers to establish a baseline average length of 10 mm; antennae whose length deviated from this length by more than 2 mm were not selected for use in the experiment and were returned to the holding containers for alternate usage. The antennae were cut at varying points with fine micro scissors (Vananas Scissors 15000-03, Fine Science Tools GmbH, Heidelberg, Germany) with the exposed ends dipped into a 10% solution of micro-Ruby (tetramethylrhodamine and biotin dextran, MW 3000, lysine fixable; Life Technologies, Oregon, USA) for one minute to allow for sufficient absorption. The subject was then moved to a refrigerator unit (4 ºC) overnight with moist cellulose paper to both allow sufficient time for transportation of dye in the sensory axons, as well as induce a narcotic state pre-dissection. The following day, the insect antennae were then measured again to confirm the initial measured distance cut was accurate, followed by the dissection procedure.

To obtain the antennae samples, two subjects had their antennae removed whole at the pedicel with micro scissors and placed into the fixation solution to later be scanned with the

confocal microscope. The insects that the antennae samples were retrieved from were then returned to the insect containment cylinders to live out the rest of their natural lifespan.

[2.3] Insect brain dissection and dehydration

Decapitation was performed first with micro scissors and the subject's head was then firmly affixed with melted utility wax to the bottom of a well. Once the wax dried, the well was filled with Ringer solution (in mM: 150 NaCl, 3 CaCl2, 2 KCl, 25 sucrose, & 10 N-tris (hydroxymethyl)-methyl-2-amino-ethanesulfonic acid, pH 6.9) to prevent desiccation. The cephalic scales were removed with a cotton swab, and the dorsal head cuticle and ommatidia were cut into with a razor knife and removed with fine forceps. The ocular fluid was absorbed by a small cotton swab. The proboscis and mandibles were cut with micro scissors and removed with fine forceps, followed by the muscle and trachea. After successful dissection of the brain from the head capsule, the brain was transferred to an Eppendorf tube containing a 04% paraformaldehyde fixation solution to preserve the sample, prevent decomposition, and to increase the tissue's mechanical integrity and resilience for the dehydration procedure.

After fixation in the 04% paraformaldehyde solution for one hour, the samples were dehydrated in an ascending ethanol series (50%, 70%, 90%, 96%, 2 x 100% ethanol. 10 minutes each). During both fixation and dehydration, the samples were shielded from light atop a platform shaker (Rotomax 120, Heidolph Instruments, Kelheim, Germany). They were then rinsed with, and stored in, methyl salicylate (oil of wintergreen, C8H8O3) serving dual clearing and storage purposes until scanning, wherein they were transferred between two glass cover slides placed upon a 1 mm thick aluminum metal slide well, also filled with methyl salicylate, for confocal microscopy. The samples were orientated under a microscope with fine forceps to a frontal view to allow for the best scanning angle for the antennal lobes.

[2.4] Confocal Image Acquisition

Sample preparations were scanned at NTNU's Center for Advanced Microscopy, an interdepartmental collaboration at NTNU's Gløshaugen campus. All samples were scanned and imaged using two channels in a confocal laser microscope (Zeiss LSM 800, Jena, Germany). An EC Plan Neofluar 20x/0.5 air objective was used to scan the antennal lobes, and a C-Apochromat 10x/0.45 water objective was used to scan the antennae. In one channel, the neurons labeled with micro-Ruby dye (Excitation 555 nm / Emission 580 nm) were excited by a 553 nm helium-neon laser, with emissions collected by a 568 nm long-pass filter

(detection wavelength 570-601 nm). In the other channel, the autofluorescence of the sample tissue was excited by a 493 nm argon laser, with emissions captured by a 517 nm band pass filter (detection wavelength 410-546 nm). The pinhole size was set to 1 airy unit. The optical slice distance was between 1-3 μm for antennal lobe scans (set to 30% overlap), and 7.10-7.20 μm for the antennae sections. Image resolution was set to 1024 x 1024 pixels, and scan speed was set to 5. The images were acquired and processed using the software ZEN 2 (blue edition, Carl Zeiss Microscopy GmbH, Jena, Germany).

[2.5] Data Preparation

Scans were categorized into proximal (0.0 mm – 2.9 mm), medial (3 mm – 6.9 mm), and distal (7.0 mm and above) for analysis. For digital reconstructions of the AL glomeruli, the raw confocal image stack data were converted from .czi files to .lsm files with ZEN black (ZEN 2.3 SP1 (black edition); Carl Zeiss Microscopy GmbH, Jena, Germany) for use in Amira 6.0 (Konrad-Zuse-Zentrum für Informationstechnik Berlin and FEI SAS, Berlin, Germany). To keep the innervation selection equal across the different samples, the .czi files were first processed in Fiji (Schindelin et al., 2012). The brightness was auto adjusted utilizing the "stack contrast adjustment" plugin (Capek et al., 2006) to equalize brightness across the stack, and then the contrast was adjusted utilizing the *Image/Adjust/Threshold* function with the "stack histogram" box checked, with the "auto" selection to keep the selection process equal across the different samples. Finally, the images were saved as a .tiff image file to use in Amira.

[2.6] Digital Reconstruction and Volumetric Analysis

The glomeruli were manually demarcated using the paint brush tool across three spatial planes, before the wrap selection filter was used to mark most of the glomerular space. Afterwards, the glomeruli boundaries across each Z-frame were individually touched up, having necessary areas removed or added. After the glomeruli boundary data were obtained and saved in a label data file, the file was duplicated to resume working on the innervation portion, ensuring the spatial area of the innervated portions matched the spatial area of the glomerular portions. The innervation data at this point was averaged and auto-adjusted to have values of zero or one; the zero areas were removed, and the remaining selection was the accepted innervation input data. The files were then downsampled (*Compute/Resample* from 2, 2, 1 to 4, 4, 2), had a surface generated (*Compute/Generate Surface*), had their surface

smoothed (*Compute/Smooth Surface*, 20 iterations with lambda 0.6), and were transformed by a magnitude of 1.54 across the Z-axis to compensate for the refraction difference due to using an air objective with a sample immersed in methyl salicylate. The volume of the glomeruli and innervation were measured by the material statistics function (*Measure and Analyze/Material statistics*) after Z-axis transformation. The AL files were opened without further change in Amira 5.3 (Konrad-Zuse-Zentrum für Informationstechnik Berlin and FEI SAS, Berlin, Germany) to export images. The insect antennae scans were opened in ZEN blue to create maximum intensity projection images. All images were processed in GIMP 2.10.

[2.7] Ethics

Directive 2010/63/EU *on the protection of animals used for scientific purposes*, recently amended in 2019 by Regulation (EU) 2019/1010, gives legal protections only to live non-human vertebrate animals and one class of invertebrates, Cephalopoda. The most recent Norwegian Animal Welfare Act (Dyrevelferdsloven replaced Dyrevernlova in 2010) adds further protections for three arthropods: the crayfish, the squid, and the honeybee. *Lepidoptera* bear no current restrictions nor protections in their usage in research or handling. Nevertheless, care was utilized in their handling and termination to minimize subject stress and suffering, and animal habitats were checked and cleaned daily. From the scientific perspective, healthy animals ensure accurate and reliable data. From the philosophical perspective, in acknowledgement of universal ethics, all creatures deserve a level of consideration.

[3] Results

Of the 53 stained preparations, 21 were successful in providing intact stained ALs. Confocal scans of these preparations were retrieved and analyzed. The data was categorized into basal, medial, or distal based on the antennal site of dye application. From these 21 confocal stacks, three were chosen to serve as representative samples for Amira reconstruction. The varying proximal-distal amputations revealed several discernable trends concerning projection patterns in the AL glomeruli. An example of the corresponding innervation and antennal bisection points can be seen below in Figure 3.

The term “innervation value” (IV) will be utilized from this point forward, to be defined as “the volume of the area stained by the dye carried by the OSNs, divided by the volume of the entire glomeruli”, e.g., the proximal IV refers to the innervation ratio calculated from the proximal cut sample.

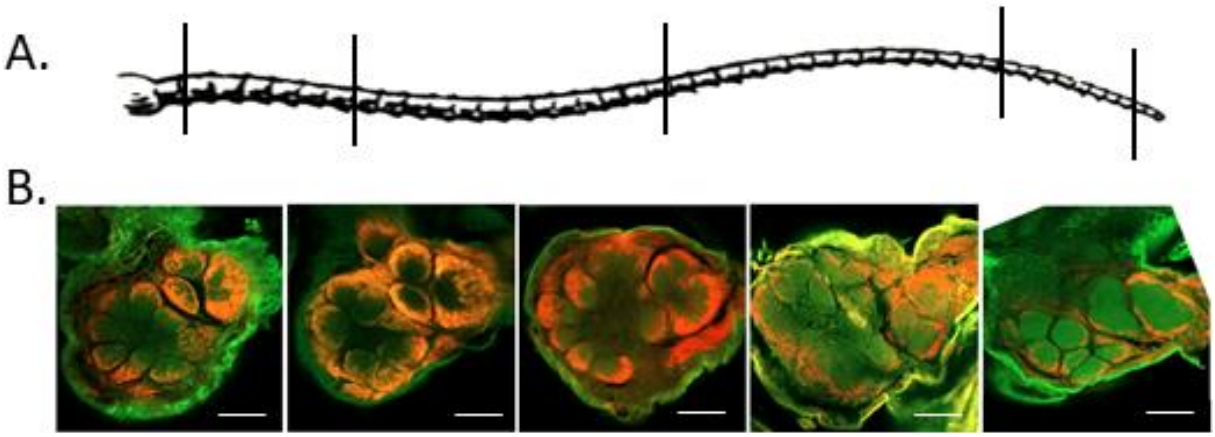

Figure 3: **Antennal bisection points and the corresponding glomerular innervation pattern.**
(A) Schema of an intact antenna showing amputation sites for the corresponding confocal images in (B). Amputation sites measured (in mm) 0.75, 2.00, 5.00, 8.00, 9.50 away from the base respectively.
(B) Confocal images showing approximal same depth across different samples. Scale bars are 50 µm.

[3.1] Innervation patterns from distal cut preparations

The reconstruction of the distally stained preparation (see Figure 4) revealed unexpected patterns. Rather than each part of the AL receiving equal projections from the OSNs, there are large differences between the anterior and posterior ordinary glomeruli, with heavier rates of innervation in the anterior segments. The depth of the innervation is shallow at this point, only covering some of the outer most layers, and sporadically at that, which is displayed in greater detail within Figure 5. This detail is repeated across the different experimental bisections, displaying that the more proximal cuts show a deeper and broader area of innervation. Regarding the general innervation pattern, the distally located OSNs also included a difference to according to lateral versus medial AL glomeruli. In the distal

reconstruction the lateral sides display the most striking visual example of the stronger innervation in comparison to the medial.

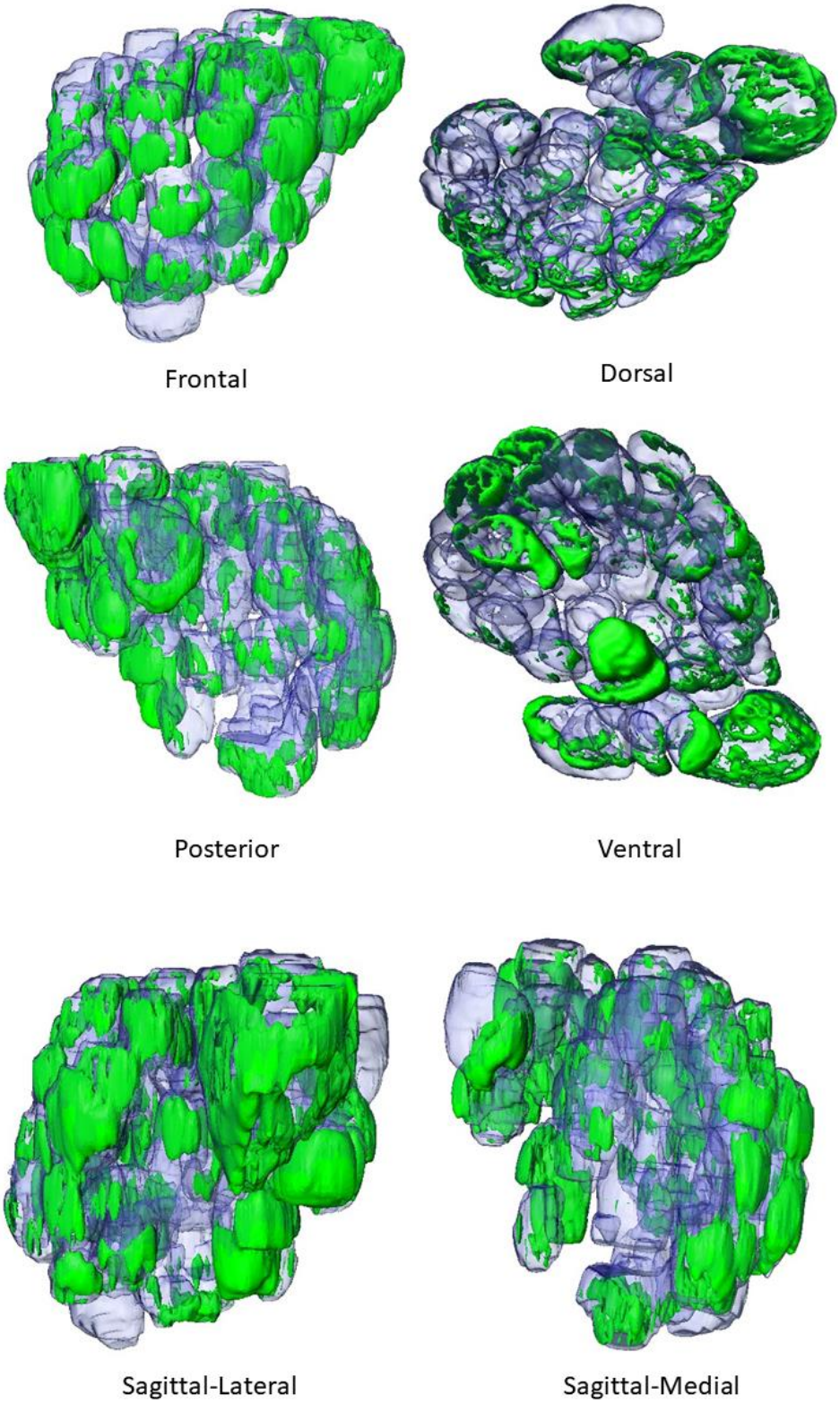

Figure 4: **Amira antennal lobe reconstruction obtained from confocal data; distal cut, 9 mm from base.** Panels show the entire lobe from various orientations. The glomeruli are displayed in 70% opacity blue to allow the innervations from the OSNs (in shaded green) to be seen. Figures are presented in perspective view.

The overall IVs for the entire AL (12%) approximately mirror the proportion of flagellum amputated (10%), however the cumulus displayed an IV of 25%. The cumulus is unique in this regard as the other two units of the MGC, the dm-a and dm-p, had IVs of 7.8% and 6.6% respectively. The IV for the entire AL is used for comparison instead of the IVs for only the ordinary glomeruli as a matter of discretion. Removing the MGC and using only OG would change the IV from 12.3% to 11.1%. Additionally, were the LPOG to be removed as another exceptional glomerulus, the IV would increase back to 12%.

Figure 5 (right) displays distinctive innervation sites within the cumulus for the relevant OSNs. Sub-compartments of the cumulus can also be seen to a degree in the autofluorescence of the left image.

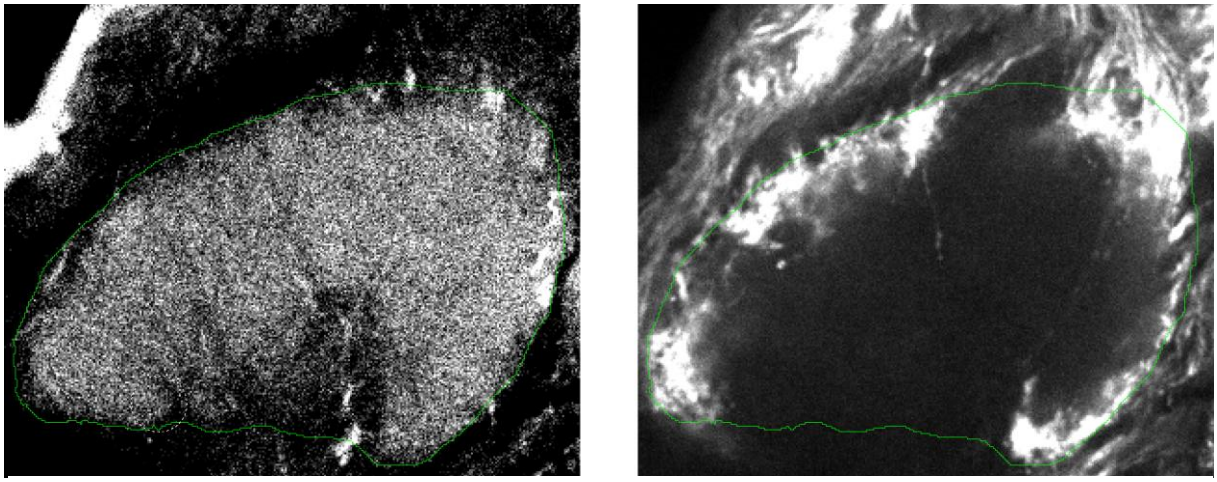

Figure 5: **Cumulus innervation from the distal cut.**
(left) Image data from the autofluorescence channel displaying the boundary of the glomerulus. (right) Image data from the dye channel displaying OSN innervation inside the cumulus.

[3.2] Innervation patterns from medial cut preparations

The glomerular innervation pattern induced by staining the OSNs from the medial part of the antenna, resulted in relatively strong staining. This can even be seen in the confocal data: a sample Z-stack frame is shown in Figure 6. But the pattern is most readily apparent in the reconstructions produced by the confocal data, seen in Figure 7.

The lateral side of the AL is moderately innervated by this point, while the medial side is still receiving sparse innervation. An exception of sorts is seen in Figure 6 for G53, which highlights that rather than the lateral-medial split being a constant gradient depending on pure geography, it is instead dependent upon the tracts innervating the glomeruli. Despite being located on the medial side, G53 receives a dedicated bundle of OSNs that split off as they travel ventrally towards the antennal mechanosensory and motor center. Glomerulus 53

belongs to a different sub-group, and thus possess a different pattern of innervation than the medial group.

The ventromedial cluster of glomeruli that were sparsely innervated at the distal cut reconstruction remain so, having still not yet received much innervation if any additional innervation. The AL reconstruction for medial antennal cut (see Figure 7) largely reinforces the previous patterns observed from the distal cut reconstructions.

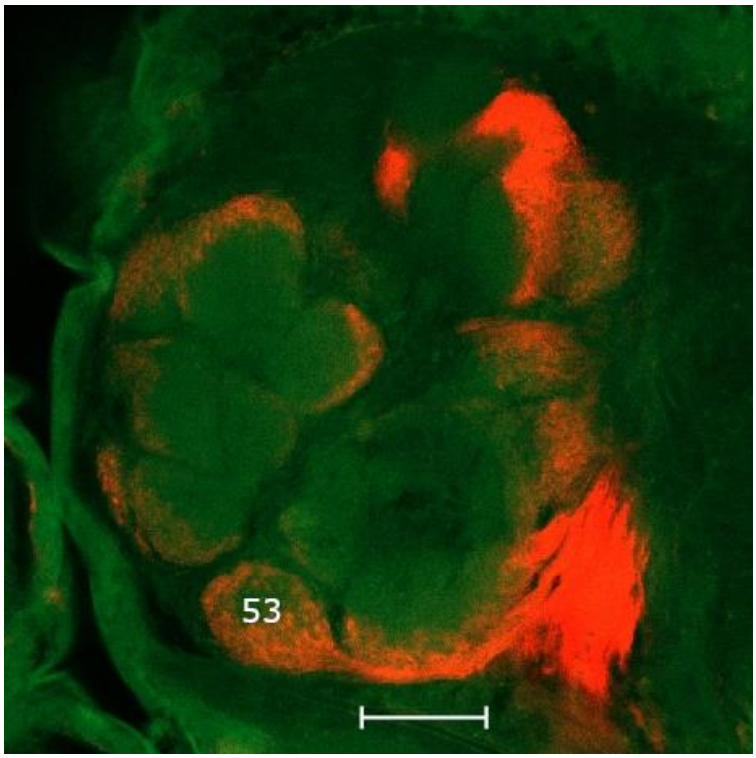

Figure 6: **Confocal image of OSN projections from the AN innervating G53.** Scale bar is 50 μm.

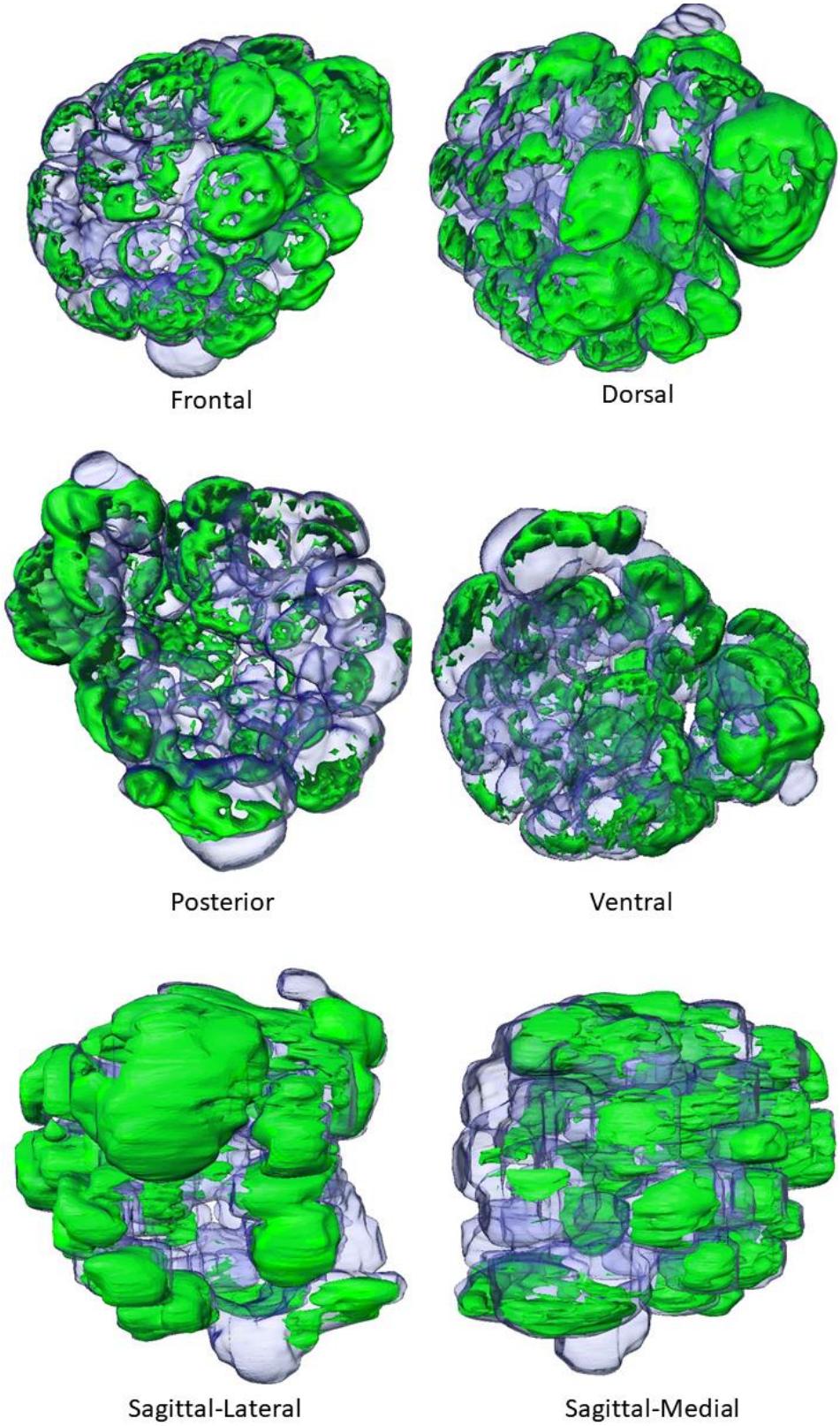

Figure 7: **Amira antennal lobe reconstruction obtained from medial cut (5mm from base) confocal data.** Panels show the entire lobe from various orientations. The glomeruli are displayed in 70% opacity blue to allow the innervations of the OSNs (in shaded green) to be seen. Figures are presented in perspective view.

[3.3] Innervation patterns from proximal cut preparations

The reconstructions for the proximal cut preparation (Figures 8 and 9) display some of the most unexpected data. Visually, most of the AL seems to be largely innervated, apart from a medially located cluster of glomeruli which correspond to G40-42 and G58-60 as identified by Zhao et al. (2016) in Figure 10. The asymmetrically sparse innervation observed for the medial cluster of glomeruli, displayed most prominently in Figure 8, was demonstrated in every sample. No significant innervation from the OSNs appeared in the medially located units in any preparation. These glomeruli returned an average proximal IV of 5%. In the Amira software, the areas corresponding to the glomerular sites receiving the innervation were so sparse it did not generate a visible surface.

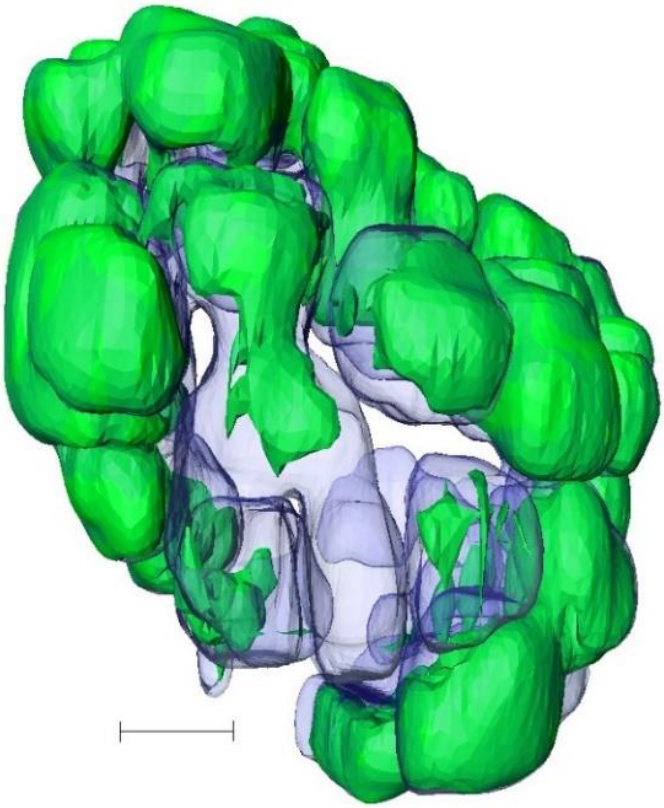

Figure 8: **Medial half of the Amira AL reconstruction obtained from proximal cut data.**
Figure shows the AL in a medial-sagittal view with the lateral half of the AL removed for visual clarity. Glomeruli are presented in transparent blue, and the OSN innervation is shown in shaded green. Scale bar is 50 μm.

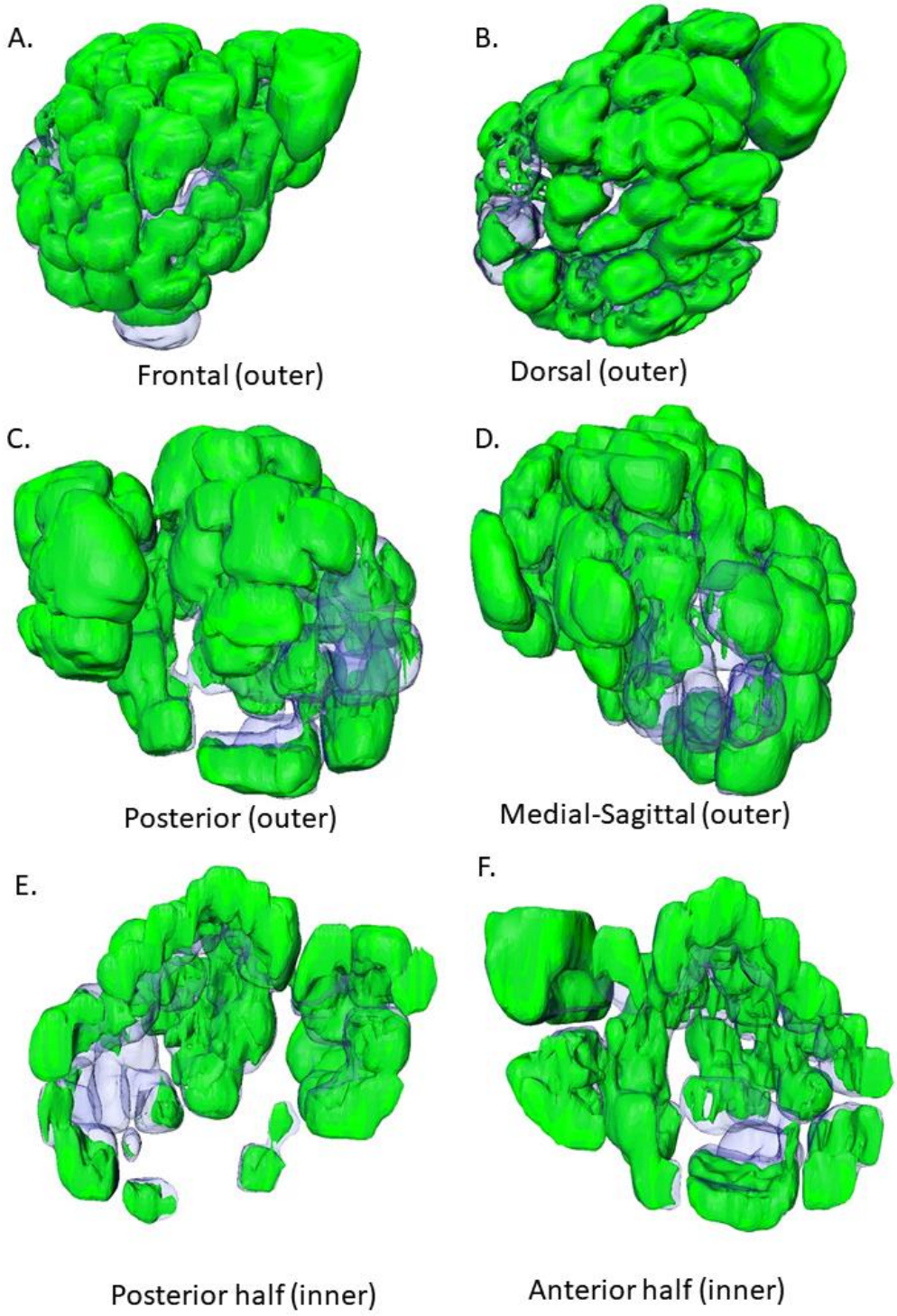

Figure 9: **Amira AL reconstruction obtained from proximal cut (0.75 mm from base) confocal data.** Panels show the AL from various orientations. The glomeruli are displayed in 70% opacity blue to allow the innervation from the OSNs (in shaded green) to be seen. Figures are presented in perspective view.
A-D show the entire AL, whereas E-F show halves of the AL: the AL was digitally cut in half and the opposing side was hidden to display the inner portions of the lobe.

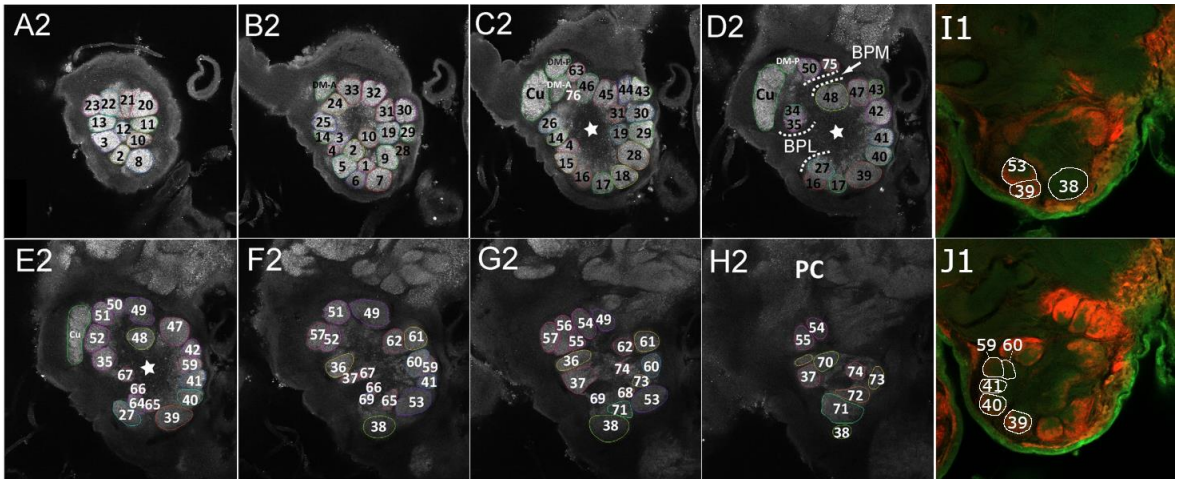

Figure 10: **Glomeruli identification.**
Panels A2-H2 adapted from Zhao et. al 2016, "The most anterior glomeruli, at 30 µm (A), 48 µm (B), 66 µm (C), 87 µm (D), 99 µm (E), 111 µm (F), 126 µm (G), and 138 µm (H)."

Panels I1 & J1: Confocal images of the AL at different depths of the AL showing OSNs (red) into the AL in the proximal-cut sample. Autofluorescence of the brain is in green. Orientation is reversed across the X-axis in comparison to Zhao et. al due to the preparation being from the alternate AL.

[3.4] General trends and exceptions

The first observable trend was for denser innervation on the lateral side of the AL in comparison to the medial side across all samples (see Figure 11). Glomeruli innervation favors placement upon the side the OSN projections approach, with most of the pathways approaching laterally directly from the antennal nerve. Alternate approaches appear to be a result of the OSN projections being required to wrap around other glomeruli to reach. The non-stained areas within the glomeruli, most often being found facing the inner core of the AL, are presumed to contain the local interneurons and projection neurons.

The LPOG is the first expected exception to the general innervation pattern, as it receives no innervation by the antennae. This allows it to serve as both a landmark and control for the mass staining of the AL (see Figure 11). The second notable deviation was the asymmetrically sparse innervation observed for a few medially located glomeruli (see Figure 9), a deviation which was repeated in every sample. These glomeruli returned an average proximal IV of 5%, which were almost all sparsely spaced enough to not have a visual surface generated from the Amira reconstruction data. The IV for these glomeruli is a deviation rather than a consequence of the first trend – the lateral side having heavier weight – as the neighboring glomeruli G39 and G53 have IVs comparable to the ordinary glomeruli average. The third notable deviation was the horseshoe group, a series of small units Zhao et al. (2016) numbered as G64-69. This cluster of small glomeruli returned a proximal IV of just under

25%, well below the proximal ordinary glomeruli IV of 64%. Similar comparative ratios were returned in the medial and distal reconstruction data.

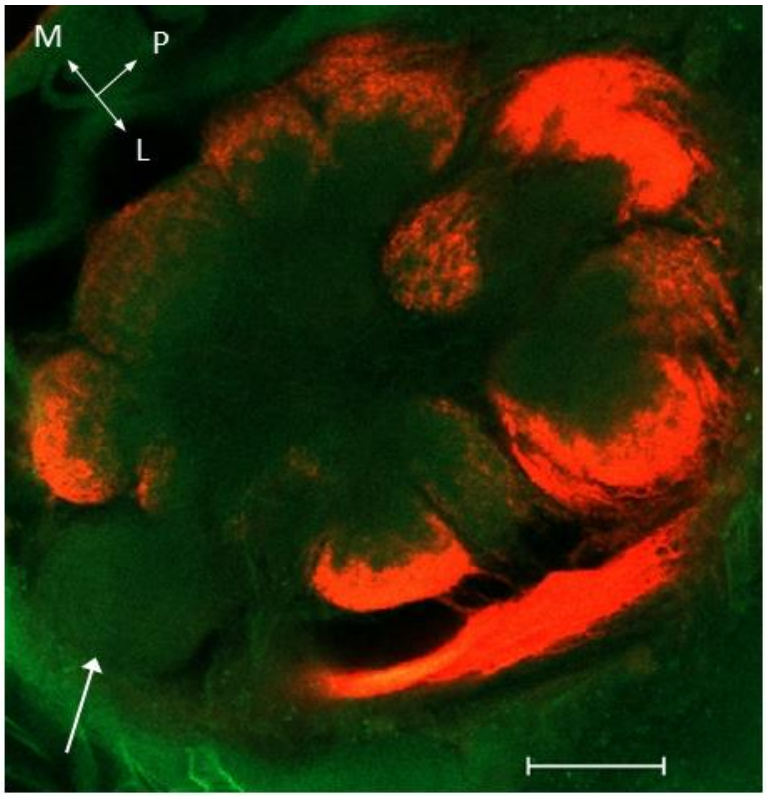

Figure 11: **Confocal image data of proximal cut sample.**
White arrow points to the LPOG. Scale bar is 50 μm.

The fourth and last notable deviation was the MGC, which in every sample displayed a disproportionately higher IV compared to the ordinary glomeruli. Within the MGC category, the cumulus at every point revealed a much higher IV in comparison to either the dm-a and dm-p. The dorsomedial units displayed varying IV comparison rates to the ordinary glomeruli depending on which proximal-distal level was being measured. These last two points show that not only is the AL glomeruli innervated distinctly depending on the site of the OSNs along the flagellum length, but that different glomeruli also seem to be innervated at different rates. At distal cuts, for example, the cumulus displayed an IV of 25%, despite the staining location being responsible for approximately 10% of the antennal length, while the dorsomedial units revealed an IV of approximately 9% at that point.

Comparisons of the IVs between the MGC units and the rest of the AL can be seen in table 1, and MGC specific reconstructions can be seen in Figure 12. Every glomerulus followed the same type of innervation pattern presented by the cumulus in Figure 12. At distal cuts, cumulus innervation is shallow and sporadic, while at medial cuts the innervation

spreads wider primarily and deeper secondarily. And even at ‘max’ innervation there remains an area empty of OSN projections, which are presumed to host processes of LNs and PNs.

Table 1: **IVs of the AL, MGC units, and OG at different proximal-distal bisection points.**
The number inside the parenthesis reflect the comparative IVs compared to their “full” proximal amounts.

Structure	Distal (10.5 -> 9.50 mm)	Medial (10 -> 5 mm)	Proximal (10 -> 0.75 mm)
Entire AL	12.29 (18.65%)	23.31 (36.19%)	64.41 (100%)
Cumulus	25.15 (28.11%)	49.90 (55.33%)	90.18 (100%)
Dm-a	7.82 (10.36%)	20.53 (27.22%)	75.42 (100%)
Dm-p	6.64 (8.65%)	28.54 (37.21%)	76.69 (100%)
Ordinary	11.12 (18.09%)	20.58 (33.49%)	61.46 (100%)

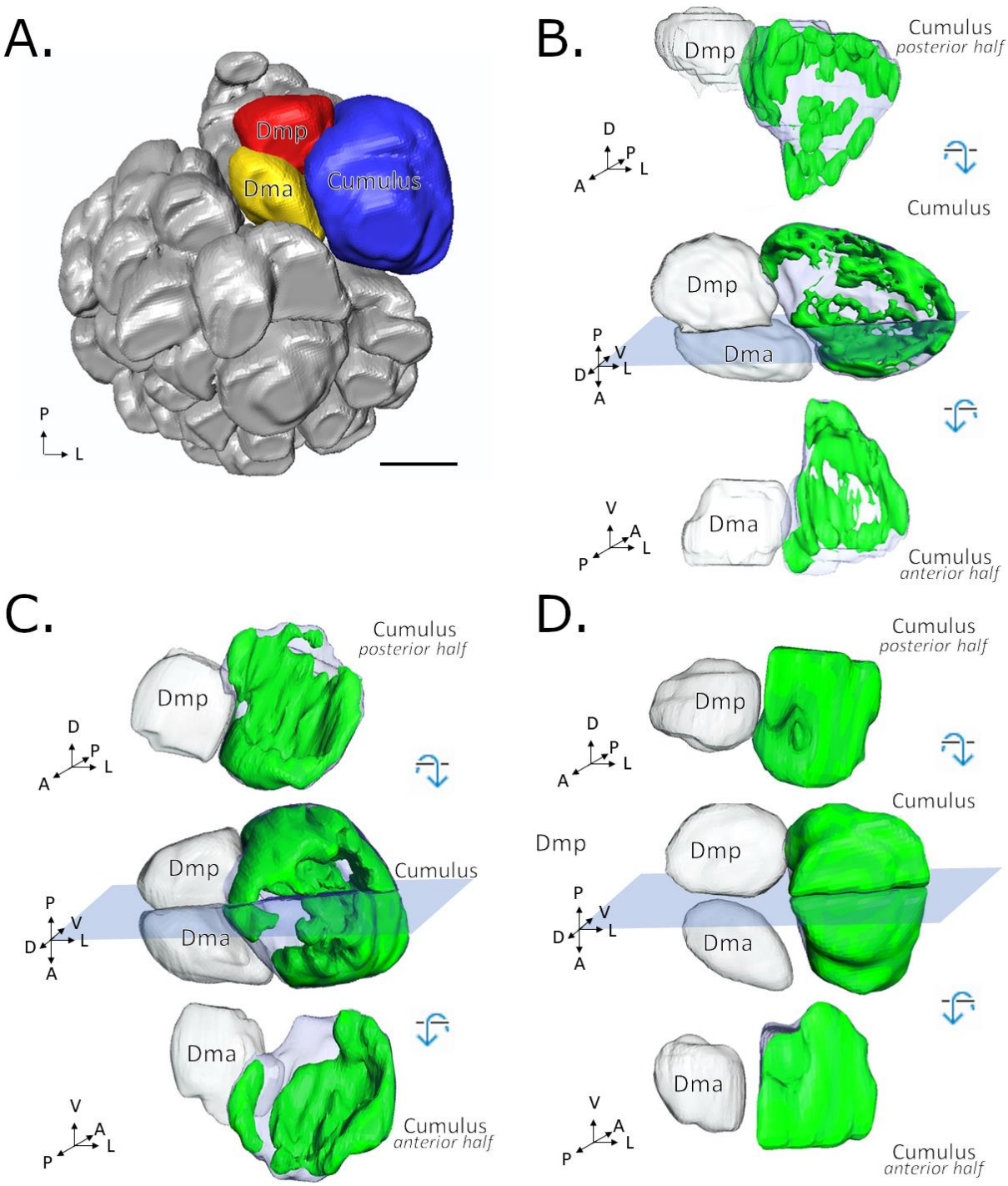

Figure 12: **Amira reconstructions showing cumulus innervation obtained from varying staining locations of the antennal OSNs.**
A: Dorsal view of the AL with the MGC glomeruli highlighted. Scale bar is 50 µm.
B-D: Cumulus innervation at distal (B), medial (C), and proximal (D) cuts. Cumulus glomeruli are displayed in transparent blue, dorsomedial units are displayed in transparent grey, and cumulus innervation is presented in shaded green.

4. Discussion

[4.1] Possible reasons for innervation differences between select glomeruli

The cumulus receives a higher proportion of innervation originating from the distal parts of the antennae in comparison to all other AL glomeruli; as seen in Figure 4, the cumulus is already moderately innervated as opposed to the comparative sparse innervation seen in the other areas. One possible explanation for this could be the location of the cumulus in relation to the AN; however, that explanation would be incorrect. It is not the case that IVs are unilaterally higher the closer they are to the AN, as the dm-a and dm-p at points have lower IVs compared to OG further away on the lateral and anterior sides, as reported in Table 1. Thus, it must be the case that location is not a determining factor of innervation.

A plausible explanation for the IV differences is due to function. At the distal cut, which corresponds to 10% of total antennal length stained, the cumulus had an IV of 25.2%. Said in another way, the cumulus in this subject constituted 9.5% of the total volume of all AL glomeruli and was receiving 19.4% of all the innervation that was being projected from the distal staining location on the periphery of the antenna. This inordinate weighing suggests that the antennae is relatively more tuned to detect pheromones in the periphery than in the proximal segments, at least regarding the number of PR OSNs – which may have also influenced the development of the long sensilla trichodea near the more proximal areas of the male noctuid moths.

Consider the nature of *H. armigera* pheromone-plume navigation. The insect has a zigzagging behavior with counterturns and casting as it attempts to locate the source of the pheromone, shown in Figure 13 (Cardé, 2019). A higher proportion of PR cells on the distal most part of the antennal periphery would enable the insect to detect and react more rapidly to the ever-changing olfactory landscape as it attempts to navigate the environment, e.g., the boundaries of the antennal plume. Long sensilla trichodea near the head results in a pseudo-wedge shape of sorts, which provides a more suitable shape for the detection of pheromones from a flittering female in flight; whereas longer sensilla trichodea at the tip would in fact work counter to its purpose. Figure 14 displays two type of simple structures, a uniform rectangle (A) and a wedge (B). While longer sensilla trichodea at the tip of the antennae would be counterproductive to fine detection, an odorant molecule narrowly missed by the most distal periphery may be picked up by the longer proximal hairs to help orient a steering direction.

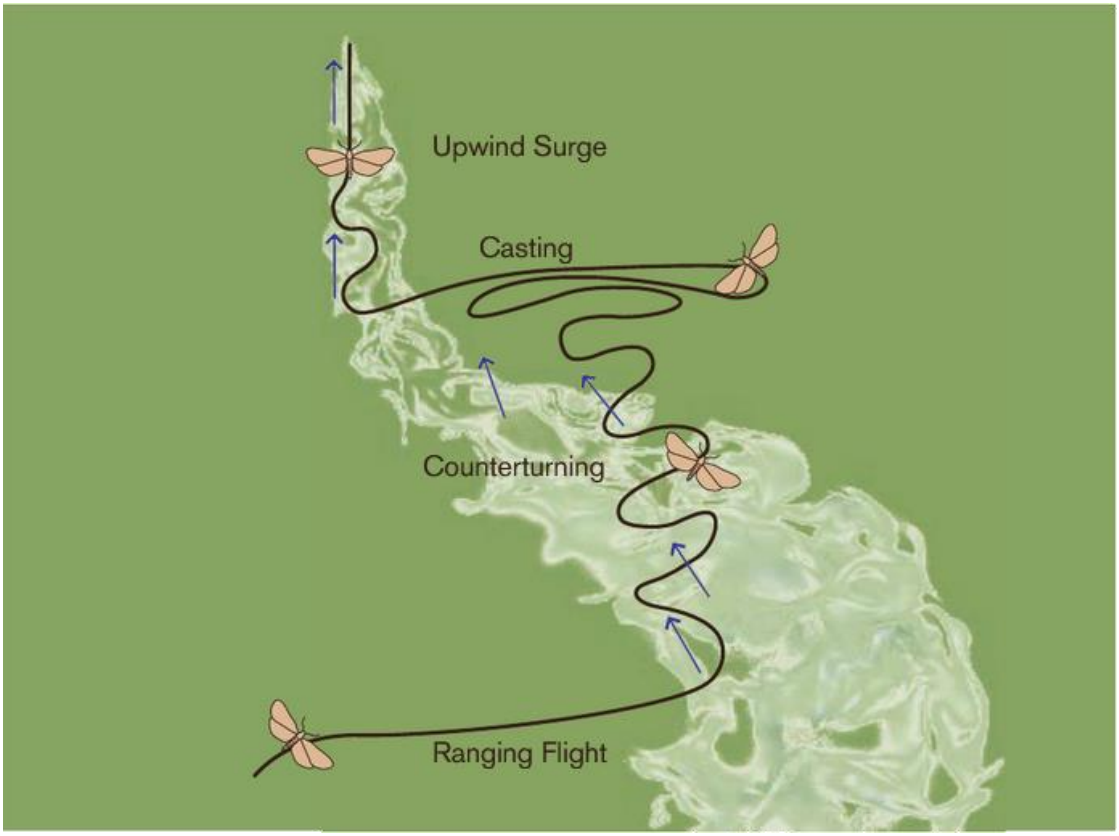

Figure 13: **Template of moth maneuvers as governed by sequential interactions with filaments of pheromone, encounters with "clean air," and wind flow.**
From (Cardé, 2019).

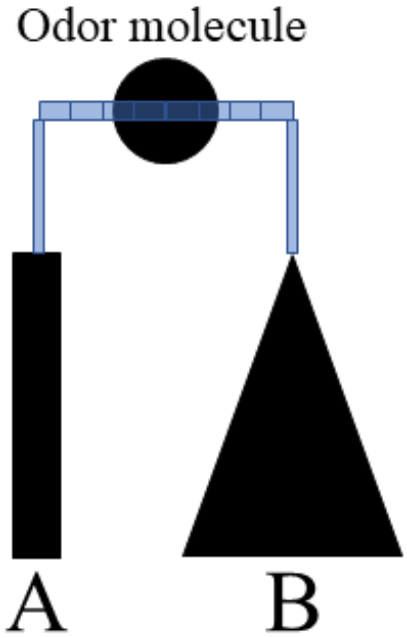

Figure 14: **Schematic of antenna shapes**
The antennae are placed equally far apart from odor molecule.
The transparent blue boxes are provided for easy visualization.

[4.2] Spatial-temporal encoding of the antennae

There are distinct innervation sites in the glomeruli which correspond to specific areas upon the antennae. Figure 5 presents a confocal image of the cumulus with innervations originating solely from the experimentally stained distal bisection point to serve as a visual example. It is plausible that the geometry of this neural circuitry is utilized as an encoding of some sort of internal spacial map for *H. armigera* and other *Noctuidae*. Such conclusions were also arrived at by Nishino et al. (2018) who performed a similar experimental flagellum amputation of the cockroach *P. americana*, with the addition of stimulus delivery recordings. Their results showed that the size and position of the pheromone stimulus is encoded in the olfactory circuit through the detection of which sensory neurons are activated along the antennae, transferring the information to the MB. The size of the pheromone stimulus Similarly, Wehr and Laurent (1996) reported that odorant information is carried not only in the specific neural assemblies activated at the moment of detection, but also in the sequence at which the assemblies update during an odor response, signifying an encoding of temporal information. Through means of the primary and secondary olfactory processing centers, the antennae convey spacial-temporal information insofar as how and where along the antennae the odorants are detected. In *P. americana*, navigation performance in cockroaches who underwent unilateral antennectomy was statistically equal to cockroaches possessing both antennae – provided the single antenna length was equal to that of the dual antennae possessing cockroaches, who otherwise had partial flagellum amputations to match the total antennae lengths (Lockey & Willis, 2015). Said another way, a loss of six millimeters of total antennal length proved equal hinderance whether the loss was distributed across one antenna or two antennae, lending credence to the antennal spatial map hypothesis.

The glomeruli of the aerial *H. armigera* receive their antennal olfactory information ipsilaterally, similarly to the terrestrial cockroach *P. americana*. The anatomical details by which *P. americana* determine odor location ultimately state cockroaches with a single antenna navigate just as well as cockroaches with both antennae (Lockey & Willis, 2015). To further draw parallels between the two species, these findings correspond to a flight behavioral study involving unilateral antennectomy with *H. virescens*. Male *H. virescens* performed observably normal flight behavior after the antennectomy and most subjects performed measurably similar pheromone tracking behavior, with a subset (36%) of moths performing slightly contextually erratic behavior in plume tracking depending upon from which side they entered the plume (Vickers & Baker, 1991). The moths belonging to the slightly eccentric subset still navigated successfully to the source of the plume, albeit with

additional zigzag and casting behaviors. This is likely explained by another behavioral noctuid flight study with *Manduca sexta*, which revealed that bilateral antennectomy abolished flight control (Sane et al., 2007). The experimental design of this study revealed that the detection of Coriolis forces by the Johnson's organ within the antennae were necessary for flight control. The *M. sexta* moths who underwent bilateral antennectomy were unable to sustain controlled flight, however reattachment of the antennae restored moderate flight control despite the no-longer-functioning AN, leading the authors of the study to determine it was the feedback obtained from the mass of the antennae itself which was a prerequisite for flight control; see Figure 15. Flight control in the study was determined by the substantially increased rates of backwards flight, crashes, and collisions. Reattachment of the antennae was achieved through simple glue, providing a weight without reestablishing sensory feedback. This lack of flight control in the *M. sexta* moths who underwent bilateral antennectomy in Sane et al. (2007) suggests that rather than an inability to navigate the odor plume due to olfactory reception, the *H. virescens* moths who underwent unilateral antennectomy and displayed slightly impaired odor tracking – measured by flight behavior – is possibly an issue of flight control instead.

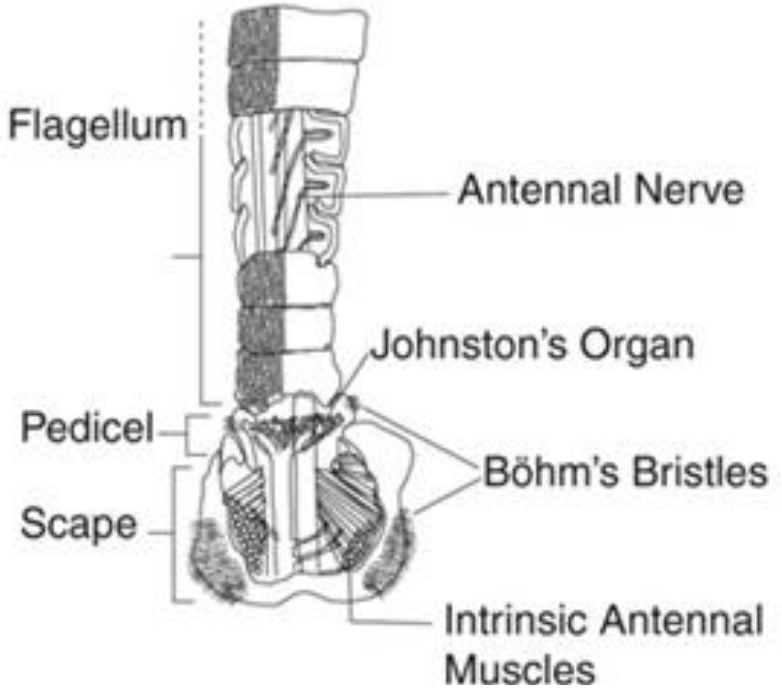

Figure 15: **Longitudinal cross section of the basal segments of the antenna.** Adapted from (Sane et al., 2007).

The findings for those species contrast with olfactory navigation studies performed with *D. melanogaster*, in which it was found that while bilateral antennal olfactory input enhances chemotaxis behavior in the larval form (Louis et al., 2008), it is required for navigation in the adult form (Duistermars et al., 2009). *Drosophila* with unilateral antennal olfactory sensilla occluded with nontoxic ultraviolet light (UV)-cured glue were unable to maintain their spatial orientation within an odor plume, nor could they temporally integrate unilateral signals to locate the odor plume; their flight control was not affected by the UV-cured glue. When combined, the results across these species point to ipsilateral antennal projections to the AL being an integral component to unilateral antennal navigation. The species *P. americana, M. sexta, H. virescens, and H. armigera* furthermore all possess similar OSN to AL glomeruli innervation patterns.

[4.3] Antennal pheromone reception across all segments

In this experiment, pheromone reception was found across the entire length of the antennal flagellum. Zhang et al. (2001) reported that in noctuid moths, pheromone receptor cells are found in the long sensilla trichodea which stand out in lateral rows upon the antennae; these long sensilla trichodea are found predominately near the proximal half of the antennae. They further report that the function of short sensilla trichodea is less well understood in *Noctuidae*. The results of the experimental staining performed here show conclusively that the sensilla which innervate the MGC are also located near the distal periphery of the antennae. Additionally, it is also likely that every segment contributes to pheromone reception, however the bisection measurements in this study were in millimeters and not segment counts, thus not every segment was checked. It is reasonable to conclude, however, that pheromone-detecting neurons are present in each antennal segment, given the role of the antennae in determining the spatial map of received stimulus.

[4.4] Possible explanation for lack of medial glomeruli innervation

In an investigative study of the anatomical organization of the AL for the fruit fly *Bactrocera dorsalis*, anterograde staining of the antenna of the maxillary pulp was performed similarly to the method utilized by Zhao et al. (2016), along with additional anterograde staining of the PNs from the MB calyx (Lin et al., 2018). Similar results were found insofar as sparse innervation of the medial group of glomeruli. The medial group of glomeruli which

was not innervated by the antennal nerve staining was, however, stained by labeling from the maxillary palp.

In *H. armigera*, CO2 is detected by the OSNs housed inside the LPO, which is located on the labial palps instead of the antennae. Guo et al. (2018) performed a transcriptome analysis on the labial palps and proboscis of *H. armigera* and found novel sensilla subtypes as well as novel OBPs and chemosensory proteins. Of the 66 detected ORs, four were previously known. HarmOrco, previously considered an atypical co-receptor, had the highest expression level in the proboscis and labial palps, and was found to be responsive to multiple plant odors. HarmOR58, previously identified as a larval antennal specific gene (Liu et al., 2014), was also found in the tested adult tissue samples, albeit with low expression levels. Constant strides are being made in furthering our understanding of the olfactory system. But what of the maxillary palps? The considerations of them being vestigial due to their small size may not necessarily be the case. Figure 16 below shows a confocal scan reconstruction of a *H. assulta* brain with the maxillary nerves are clearly visible. It is possible that OSNs project from the maxillary palps as well; the labial nerve (B) conveys sensory information to the AL despite being further away from the maxillary palp nerve (A).

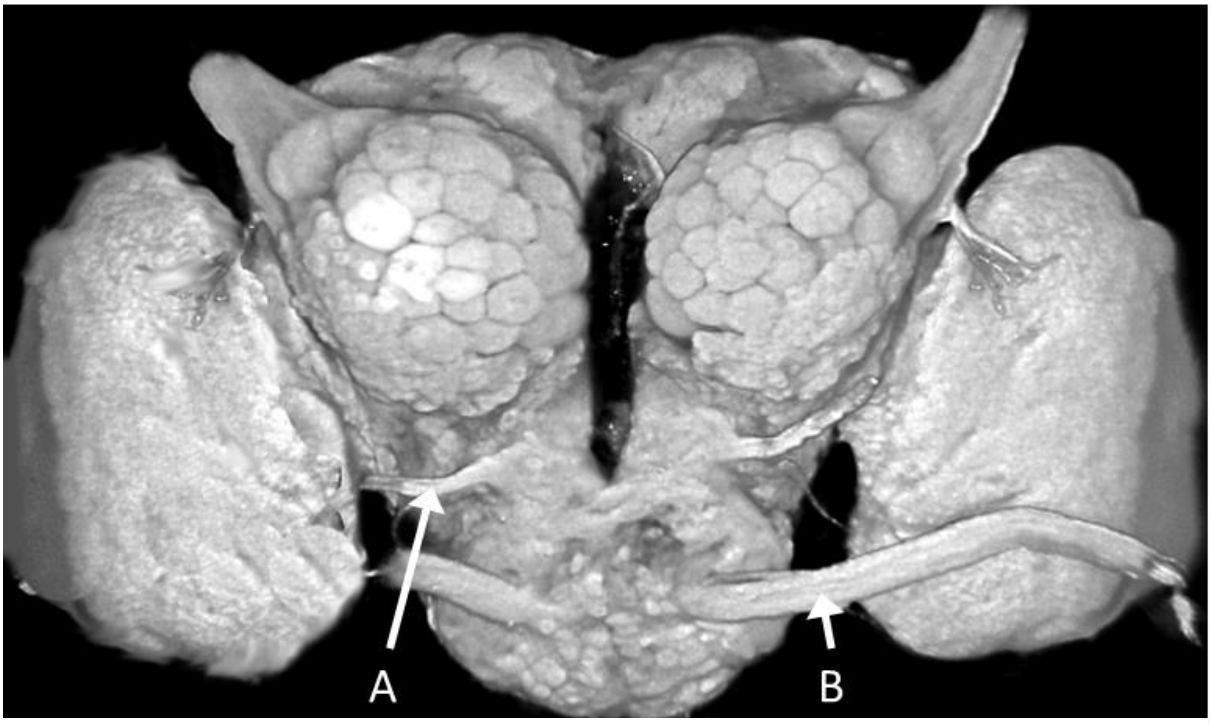

Figure 16: **Three-dimensional confocal reconstruction of male *H. assulta* brain in frontal view.**
Arrow A points to the maxillary nerve. Arrow B points to the labial nerve. Adapted from Berg et al. (2002).

Staining of *Lepidoptera* proboscises revealed termination areas of the gustatory and mechanosensitive sensilla styloconica axons in the suboesophageal ganglion area, conveyed through the maxillary nerves, but produced no innervation in the AL (Kvello et al., 2006). This eliminates in *Lepidoptera* one of the two known primary sources of innervation for the medial glomeruli in *Drosophila.* It remains to be seen what staining of the maxillary palps will reveal.

[4.5] OSN pattern similarity present in all AL glomeruli

The distal-proximal innervation pattern for the antennal glomeruli in this experiment was also found in the LPOG staining from Kc et al. (2020). They found LPO-exclusive and non-LPO sensory neurons which target the gnathal ganglion and ventral nerve core through anterograde mass-staining experiments, labeling the distal and proximal levels of the LPO. Of the LPO-exclusive sensory neurons, they found three morphological types: one bilateral, one ipsilateral, and one contralateral, with an overall projection pattern favoring the ipsilateral side. The LPOs project bilaterally to both LPOGs, with most of the innervation favoring the ipsilateral side. This contrasts with the projections from the AN, which provides solely ipsilateral projection, yet the innervation pattern of the LPOG is consistent with the rest of the AL glomeruli.

The antennal neurons arise as the antennae develop during metamorphosis. The axons of the neurons grow through the lumen of the antennae, forming a nerve that enters the AL. This fact is reflected in the occurrence of antennae grafting of moths of the opposite sex (Schneiderman et al., 1982); grafting a male antenna onto a female moth will cause the female brain to develop a normally male-specific MGC. With the LPOG seeming to share a similar innervation pattern and being part of the same AL as the rest of the glomeruli innervated by the antennae, the possibility exists that it is also created as a process of relevant OSN-triggered development. The development of glomeruli from the reception of periphery signals would thus be a characteristic of all *Lepidoptera* glomeruli instead of only those associated with the AN.

[4.6] Amira selection considerations

The numbers given for the IVs were arrived at using the automated process involving the brightness & contrast adjustment with the FIJI plugins, which was chosen to provide a measure of consistency and control across the different Z-stacks and samples. If the contrast

was adjusted per frame for optimal (human) visual clarity and the innervation was manually selected (with the paintbrush tool in Amira), the same general trend would be observed however the absolute numbers would differ. At anything that might be innervation, at the risk of mixing in autofluorescence data, giving the proximal cut as an example, AL IV is 82% (compared to processed 64%), the cumulus IV is 95% (in comparison to 90%), the medial cluster is 25% (in comparison to 04%), and the horseshoe group is 52% (in comparison to 24%). An alternate method of selection would return the same trends and exceptions to the trends, if not the same numbers; on the same hand, hand selection does not allow for comparable numbers as each frame and sample would be decided upon arbitrary means.

Very minor amounts of dye presence were tolerated as artifacts of the automatic brightness and contrast adjustment process. With a low enough sensitivity even the fluorescence of the sample tissue itself would register. A confocal example of white levels is presented in Figure 17, e.g., the LPOG (identified with a white arrow) has 1% dye presence.

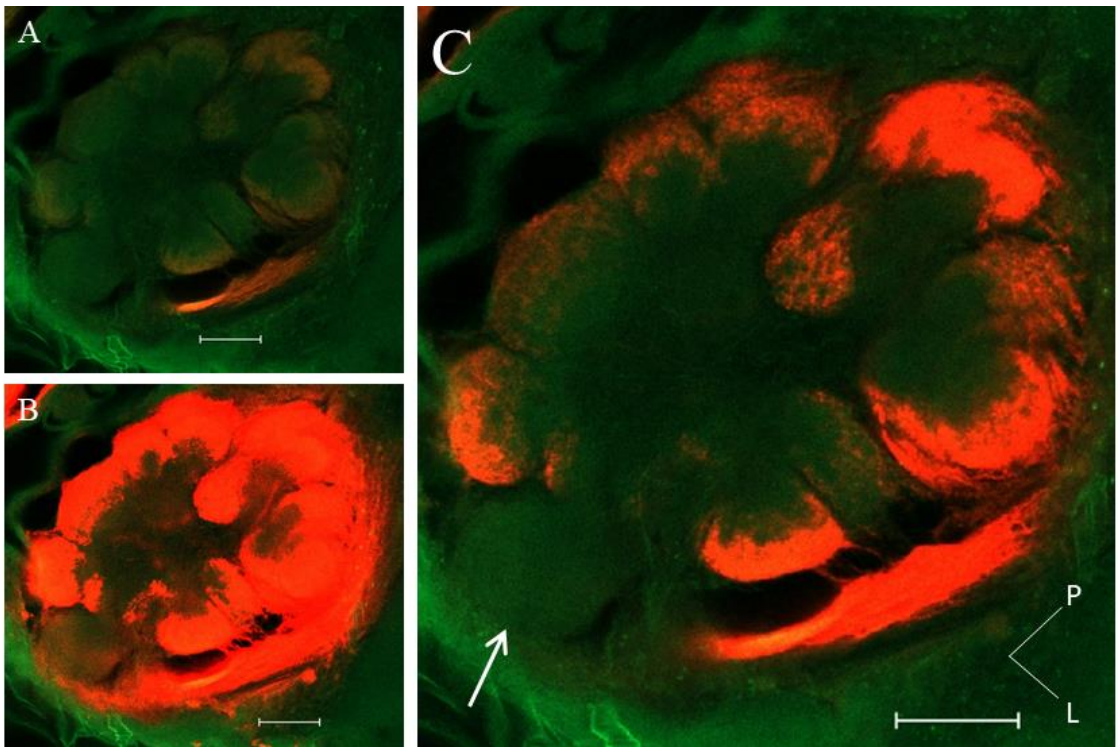

Figure 17: **Confocal image data of proximal-cut staining with different dye channel white levels.**
A: Default white level of 255. Scale bar is 50 µm.
B: White level of 10. Scale bar is 50 µm.
C: White level of 50. White arrow points to the LPOG. Scale bar is 50 µm.

Conclusions

- The findings presented here confirm previous data reporting about the projections of antennal OSNs into the ipsilateral AL glomeruli in *Noctuidae*.
- Systematic mass staining from different antennal segments of the male *H. armigera* indicate that pheromone reception occurs along the entire antennae. It is noteworthy that there seems to be a relatively higher proportion of OSNs tuned to the primary pheromone component at the periphery of the antenna than at the base – demonstrated by a relatively stronger innervation in the cumulus when staining from the periphery.
- There is a very high OSN innervation in the cumulus in comparison to the rest of the AL glomeruli, regardless of staining location.
- There is a considerably lower level of antennal OSN innervation for multiple medial glomeruli in the AL than most of the other OG, regardless of flagellum staining location.
- There is also a low OSN innervation level in the horseshoe complex (an assembly of small, posteriorly located AL glomeruli) in comparison to the rest of the OG, regardless of staining location.
- The dm-a and dm-p units of the MGC vary in their level of innervation in comparison to the rest of the AL glomeruli depending on staining location, from under the AL average at the periphery to over the AL average at proximal locations.
- Generally, the innervations from OSNs located on the peripheral part of the antenna cover the outer part of the glomeruli while OSNs located more proximally innervate gradually deeper regions.
- The systematic mass staining at different antennal segments reveals a pattern of glomerular innervation indicating an element of spatial olfactory encoding.
- These results are consistent with other findings suggesting the antennae encode spatial information relating to odorants from where upon the antennae the odorants are detected.

References

Almaas, T. J., & Mustaparta, H. (1991). Heliothis virescens: Response characteristics of receptor neurons in Sensilla Trichodea type 1 and type 2. *J Chem Ecol*, *17*(5), 953-972. https://doi.org/10.1007/BF01395602

Ando, T., Sekine, S., Inagaki, S., Misaki, K., Badel, L., Moriya, H., Sami, M. M., Itakura, Y., Chihara, T., Kazama, H., Yonemura, S., & Hayashi, S. (2019). Nanopore Formation in the Cuticle of an Insect Olfactory Sensillum. *Curr Biol*, *29*(9), 1512-1520 e1516. https://doi.org/10.1016/j.cub.2019.03.043

Anton, S., & Hansson, B. S. (1995). Sex-Pheromone and Plant-Associated Odor Processing in Antennal Lobe Interneurons of Male Spodoptera-Littoralis (Lepidoptera, Noctuidae). *Journal of Comparative Physiology a-Sensory Neural and Behavioral Physiology*, *176*(6), 773-789. https://doi.org/10.1007/BF00192625

Anton, S., & Homberg, U. (1999). Antennal Lobe Structure. In B. S. Hansson (Ed.), *Insect Olfaction* (pp. 97-124). Springer Berlin Heidelberg. https://doi.org/10.1007/978-3-662-07911-9_5

Aprotosoaie, A. C., Hancianu, M., Costache, I. I., & Miron, A. (2014). Linalool: a review on a key odorant molecule with valuable biological properties. *Flavour and Fragrance Journal*, *29*(4), 193-219. https://doi.org/10.1002/ffj.3197

Bartelt, R. J., Schaner, A. M., & Jackson, L. L. (1985). cis-Vaccenyl acetate as an aggregation pheromone inDrosophila melanogaster. *J Chem Ecol*, *11*(12), 1747-1756. https://doi.org/10.1007/BF01012124

Benton, R., Sachse, S., Michnick, S. W., & Vosshall, L. B. (2006). Atypical membrane topology and heteromeric function of Drosophila odorant receptors in vivo. *PLoS Biol*, *4*(2), e20. https://doi.org/10.1371/journal.pbio.0040020

Berg, B. G., Almaas, T. J., Bjaalie, J. G., & Mustaparta, H. (1998). The macroglomerular complex of the antennal lobe in the tobacco budworm moth Heliothis virescens: specified subdivision in four compartments according to information about biologically significant compounds. *Journal of Comparative Physiology A*, *183*(6), 669-682. https://doi.org/10.1007/s003590050290

Berg, B. G., Almaas, T. J., Bjaalie, J. G., & Mustaparta, H. (2005). Projections of male-specific receptor neurons in the antennal lobe of the Oriental tobacco budworm moth, Helicoverpa assulta: a unique glomerular organization among related species. *Journal of Comparative Neurology*, *486*(3), 209-220. https://doi.org/10.1002/cne.20544

Berg, B. G., Galizia, C. G., Brandt, R., & Mustaparta, H. (2002). Digital atlases of the antennal lobe in two species of tobacco budworm moths, the Oriental Helicoverpa assulta (male) and the American Heliothis virescens (male and female). *Journal of Comparative Neurology*, *446*(2), 123-134. https://doi.org/10.1002/cne.10180

Berg, B. G., Zhao, X. C., & Wang, G. (2014). Processing of Pheromone Information in Related Species of Heliothine Moths. *Insects*, *5*(4), 742-761. https://doi.org/10.3390/insects5040742

Capek, M., Janacek, J., & Kubinova, L. (2006). Methods for compensation of the light attenuation with depth of images captured by a confocal microscope. *Microsc Res Tech*, *69*(8), 624-635. https://doi.org/10.1002/jemt.20330

Cardé, R. T. (2019). 11. Moth Navigation along Pheromone Plumes. In J. T. Allison & R. T. Cardé (Eds.), *Pheromone Communication in Moths* (pp. 173-190). University of California Press. https://doi.org/10.1525/9780520964433-012

Chang, H., Liu, Y., Ai, D., Jiang, X., Dong, S., & Wang, G. (2017). A Pheromone Antagonist Regulates Optimal Mating Time in the Moth Helicoverpa armigera. *Curr Biol*, *27*(11), 1610-1615 e1613. https://doi.org/10.1016/j.cub.2017.04.035

Christensen, T. (2002). Pheromonal and host-odor processing in the insect antennal lobe: how different? *Current Opinion in Neurobiology*, *12*(4), 393-399. https://doi.org/10.1016/s0959-4388(02)00336-7
Christensen, T. A., Waldrop, B. R., Harrow, I. D., & Hildebrand, J. G. (1993). Local interneurons and information processing in the olfactory glomeruli of the moth Manduca sexta. *Journal of Comparative Physiology A*, *173*(4), 385-399. https://doi.org/10.1007/BF00193512
Davis, R. L. (1993). Mushroom bodies and Drosophila learning. *Neuron*, *11*(1), 1-14. https://doi.org/10.1016/0896-6273(93)90266-t
de Belle, J. S., & Heisenberg, M. (1994). Associative odor learning in Drosophila abolished by chemical ablation of mushroom bodies. *Science*, *263*(5147), 692-695. https://doi.org/10.1126/science.8303280
Diongue, A., Yang, J. T., & Lai, P. Y. (2013). Biomorphometric characteristics of different types of sensilla detected on the antenna of Helicoverpa armigera by scanning electron microscopy. *Journal of Asia-Pacific Entomology*, *16*(1), 23-28. https://doi.org/10.1016/j.aspen.2012.09.001
Duistermars, B. J., Chow, D. M., & Frye, M. A. (2009). Flies require bilateral sensory input to track odor gradients in flight. *Curr Biol*, *19*(15), 1301-1307. https://doi.org/10.1016/j.cub.2009.06.022
Duistermars, B. J., & Frye, M. A. (2010). Multisensory integration for odor tracking by flying Drosophila: Behavior, circuits and speculation. *Commun Integr Biol*, *3*(1), 60-63. https://doi.org/10.4161/cib.3.1.10076
Fitt, G. P. (1989). The Ecology of Heliothis Species in Relation to Agroecosystems. *Annu Rev Entomol*, *34*(1), 17-52. https://doi.org/10.1146/annurev.en.34.010189.000313
Frank, D. D., Enjin, A., Jouandet, G. C., Zaharieva, E. E., Para, A., Stensmyr, M. C., & Gallio, M. (2017). Early Integration of Temperature and Humidity Stimuli in the Drosophila Brain. *Curr Biol*, *27*(15), 2381-2388 e2384. https://doi.org/10.1016/j.cub.2017.06.077
Galizia, C. G., & Rossler, W. (2010). Parallel olfactory systems in insects: anatomy and function. *Annu Rev Entomol*, *55*(1), 399-420. https://doi.org/10.1146/annurev-ento-112408-085442
Guerenstein, P. G., & Hildebrand, J. G. (2008). Roles and effects of environmental carbon dioxide in insect life. *Annu Rev Entomol*, *53*(1), 161-178. https://doi.org/10.1146/annurev.ento.53.103106.093402
Guo, M., Chen, Q., Liu, Y., Wang, G., & Han, Z. (2018). Chemoreception of Mouthparts: Sensilla Morphology and Discovery of Chemosensory Genes in Proboscis and Labial Palps of Adult Helicoverpa armigera (Lepidoptera: Noctuidae). *Front Physiol*, *9*, 970. https://doi.org/10.3389/fphys.2018.00970
Gupta, N., & Stopfer, M. (2012). Functional analysis of a higher olfactory center, the lateral horn. *J Neurosci*, *32*(24), 8138-8148. https://doi.org/10.1523/JNEUROSCI.1066-12.2012
Haile, F., Nowatzki, T., Storer, N., & Davis, J. (2021). Overview of Pest Status, Potential Risk, and Management Considerations of Helicoverpa armigera (Lepidoptera: Noctuidae) for U.S. Soybean Production. *Journal of Integrated Pest Management*, *12*(1). https://doi.org/10.1093/jipm/pmaa030
Hallberg, E., & Hansson, B. S. (1999). Arthropod sensilla: morphology and phylogenetic considerations. *Microsc Res Tech*, *47*(6), 428-439. https://doi.org/10.1002/(SICI)1097-0029(19991215)47:6<428::AID-JEMT6>3.0.CO;2-P

Hansson, B. S., & Stensmyr, M. C. (2011). Evolution of insect olfaction. *Neuron*, *72*(5), 698-711. https://doi.org/10.1016/j.neuron.2011.11.003
Hartenstein, V. (2005). Development of Insect Sensilla*. In L. I. Gilbert (Ed.), *Comprehensive Molecular Insect Science* (pp. 379-419). Elsevier. https://doi.org/10.1016/b0-44-451924-6/00012-0
Hildebrand, J. G., & Shepherd, G. M. (1997). Mechanisms of olfactory discrimination: converging evidence for common principles across phyla. *Annual Review of Neuroscience*, *20*, 595-631. https://doi.org/10.1146/annurev.neuro.20.1.595
Homberg, U., Montague, R. A., & Hildebrand, J. G. (1988). Anatomy of antenno-cerebral pathways in the brain of the sphinx moth Manduca sexta. *Cell Tissue Res*, *254*(2), 255-281. https://doi.org/10.1007/BF00225800
Hu, M., Zhang, C., Mu, Y., Shen, Q., & Feng, Y. (2010). Indole affects biofilm formation in bacteria. *Indian journal of microbiology*, *50*(4), 362-368. https://doi.org/10.1007/s12088-011-0142-1
Hu, P., Tao, J., Cui, M., Gao, C., Lu, P., & Luo, Y. (2016). Antennal transcriptome analysis and expression profiles of odorant binding proteins in Eogystia hippophaecolus (Lepidoptera: Cossidae). *BMC Genomics*, *17*(1), 651. https://doi.org/10.1186/s12864-016-3008-4
Hunger, T., & Steinbrecht, R. A. (1998). Functional morphology of a double-walled multiporous olfactory sensillum: the sensillum coeloconicum of Bombyx mori (Insecta, Lepidoptera). *Tissue Cell*, *30*(1), 14-29. https://doi.org/10.1016/s0040-8166(98)80003-7
Ian, E., Berg, A., Lillevoll, S. C., & Berg, B. G. (2016a). Antennal-lobe tracts in the noctuid moth, Heliothis virescens: new anatomical findings. *Cell Tissue Res*, *366*(1), 23-35. https://doi.org/10.1007/s00441-016-2448-0
Ian, E., Zhao, X. C., Lande, A., & Berg, B. G. (2016b). Individual Neurons Confined to Distinct Antennal-Lobe Tracts in the Heliothine Moth: Morphological Characteristics and Global Projection Patterns. *Front Neuroanat*, *10*(101), 101. https://doi.org/10.3389/fnana.2016.00101
Ivanovic, Z., & Vlaski-Lafarge, M. (2016). Metabolic and Genetic Features of Ancestral Eukaryotes versus Metabolism and “Master Pluripotency Genes” of Stem Cells. In Z. Ivanovic & M. Vlaski-Lafarge (Eds.), *Anaerobiosis and Stemness* (pp. 211-234). Academic Press. https://doi.org/10.1016/b978-0-12-800540-8.00011-9
Jones, W. (2013). Olfactory carbon dioxide detection by insects and other animals. *Molecules and cells*, *35*(2), 87-92. https://doi.org/10.1007/s10059-013-0035-8
Kandel, E. R., Schwartz, J. H., Jessell, T. M., Siegelbaum, S., Hudspeth, A. J., & Mack, S. (2000). *Principles of neural science* (Vol. 4). McGraw-hill New York.
Kasinger, H., Bauer, B., & Denzinger, J. (2008, 20-24 Oct. 2008). The Meaning of Semiochemicals to the Design of Self-Organizing Systems. 2008 Second IEEE International Conference on Self-Adaptive and Self-Organizing Systems, https://doi.org/10.1109/SASO.2008.51
Kaupp, U. B. (2010). Olfactory signalling in vertebrates and insects: differences and commonalities. *Nat Rev Neurosci*, *11*(3), 188-200. https://doi.org/10.1038/nrn2789
Kay, L. M., & Stopfer, M. (2006). Information processing in the olfactory systems of insects and vertebrates. *Semin Cell Dev Biol*, *17*(4), 433-442. https://doi.org/10.1016/j.semcdb.2006.04.012
Kc, P., Chu, X., Kvello, P., Zhao, X. C., Wang, G. R., & Berg, B. G. (2020). Revisiting the Labial Pit Organ Pathway in the Noctuid Moth, Helicoverpa armigera. *Front Physiol*, *11*, 202. https://doi.org/10.3389/fphys.2020.00202

Kehat, M., & Dunkelblum, E. (1990). Behavioral responses of maleHeliothis armigera (Lepidoptera: Noctuidae) moths in a flight tunnel to combinations of components identified from female sex pheromone glands. *Journal of Insect Behavior*, *3*(1), 75-83. https://doi.org/10.1007/bf01049196

Kent, K. S., Harrow, I. D., Quartararo, P., & Hildebrand, J. G. (1986). An accessory olfactory pathway in Lepidoptera: the labial pit organ and its central projections in Manduca sexta and certain other sphinx moths and silk moths. *Cell Tissue Res*, *245*(2), 237-245. https://doi.org/10.1007/BF00213927

Klinner, C. F., Konig, C., Missbach, C., Werckenthin, A., Daly, K. C., Bisch-Knaden, S., Stengl, M., Hansson, B. S., & Grosse-Wilde, E. (2016). Functional Olfactory Sensory Neurons Housed in Olfactory Sensilla on the Ovipositor of the Hawkmoth Manduca sexta. *Frontiers in Ecology and Evolution*, *4*. https://doi.org/10.3389/fevo.2016.00130

Kohli, P., Soler, Z. M., Nguyen, S. A., Muus, J. S., & Schlosser, R. J. (2016). The Association Between Olfaction and Depression: A Systematic Review. *Chem Senses*, *41*(6), 479-486. https://doi.org/10.1093/chemse/bjw061

Kurtovic, A., Widmer, A., & Dickson, B. J. (2007). A single class of olfactory neurons mediates behavioural responses to a Drosophila sex pheromone. *Nature*, *446*(7135), 542-546. https://doi.org/10.1038/nature05672

Kvello, P., Almaas, T. J., & Mustaparta, H. (2006). A confined taste area in a lepidopteran brain. *Arthropod Struct Dev*, *35*(1), 35-45. https://doi.org/10.1016/j.asd.2005.10.003

Kymre, J. H., Berge, C. N., Chu, X., Ian, E., & Berg, B. G. (2021). Antennal-lobe neurons in the moth Helicoverpa armigera: Morphological features of projection neurons, local interneurons, and centrifugal neurons. *Journal of Comparative Neurology*, *529*(7), 1516-1540. https://doi.org/10.1002/cne.25034

Laurent, G. (1999). A systems perspective on early olfactory coding. *Science*, *286*(5440), 723-728. https://doi.org/10.1126/science.286.5440.723

Law, J. H., & Regnier, F. E. (1971). Pheromones. *Annu Rev Biochem*, *40*(1), 533-548. https://doi.org/10.1146/annurev.bi.40.070171.002533

Lee, S. G., Carlsson, M. A., Hansson, B. S., Todd, J. L., & Baker, T. C. (2006). Antennal lobe projection destinations of Helicoverpa zea male olfactory receptor neurons responsive to heliothine sex pheromone components. *J Comp Physiol A Neuroethol Sens Neural Behav Physiol*, *192*(4), 351-363. https://doi.org/10.1007/s00359-005-0071-8

Lin, T., Li, C., Liu, J., Smith, B. H., Lei, H., & Zeng, X. (2018). Glomerular Organization in the Antennal Lobe of the Oriental Fruit Fly Bactrocera dorsalis. *Front Neuroanat*, *12*, 71. https://doi.org/10.3389/fnana.2018.00071

Liu, N. Y., Xu, W., Papanicolaou, A., Dong, S. L., & Anderson, A. (2014). Identification and characterization of three chemosensory receptor families in the cotton bollworm Helicoverpa armigera. *BMC Genomics*, *15*(1), 597. https://doi.org/10.1186/1471-2164-15-597

Lledo, P. M., Gheusi, G., & Vincent, J. D. (2005). Information processing in the mammalian olfactory system. *Physiological Reviews*, *85*(1), 281-317. https://doi.org/10.1152/physrev.00008.2004

Lockey, J. K., & Willis, M. A. (2015). One antenna, two antennae, big antennae, small: total antennae length, not bilateral symmetry, predicts odor-tracking performance in the American cockroach Periplaneta americana. *J Exp Biol*, *218*(Pt 14), 2156-2165. https://doi.org/10.1242/jeb.117721

Lopez-Incera, A., Nouvian, M., Ried, K., Muller, T., & Briegel, H. J. (2021). Honeybee communication during collective defence is shaped by predation. *BMC Biol*, *19*(1), 106. https://doi.org/10.1186/s12915-021-01028-x

Louis, M., Huber, T., Benton, R., Sakmar, T. P., & Vosshall, L. B. (2008). Bilateral olfactory sensory input enhances chemotaxis behavior. *Nat Neurosci*, *11*(2), 187-199. https://doi.org/10.1038/nn2031

Löfstedt, C., Herrebout, W. M., & Menken, S. B. J. (1991). Sex pheromones and their potential role in the evolution of reproductive isolation in small ermine moths (Yponomeutidae). *CHEMOECOLOGY*, *2*(1), 20-28. https://doi.org/10.1007/bf01240662

Mayer, M. S., Mankin, R. W., & Carlysle, T. C. (1981). External Antennal Morphometry of Trichoplusia Ni (Hubner) (Lepidoptera, Noctuidae). *International Journal of Insect Morphology & Embryology*, *10*(3), 185-201. https://doi.org/10.1016/S0020-7322(81)80008-6

Meiners, T., & Hilker, M. (2000). Induction of plant synomones by oviposition of a phytophagous insect. *J Chem Ecol*, *26*(1), 221-232. https://doi.org/10.1023/A:1005453830961

Mustaparta, H. (2002). Encoding of plant odour information in insects: peripheral and central mechanisms. *Entomologia Experimentalis et Applicata*, *104*(1), 1-13. https://doi.org/10.1046/j.1570-7458.2002.00985.x

Nishino, H., Iwasaki, M., Paoli, M., Kamimura, I., Yoritsune, A., & Mizunami, M. (2018). Spatial Receptive Fields for Odor Localization. *Curr Biol*, *28*(4), 600-608 e603. https://doi.org/10.1016/j.cub.2017.12.055

Pogue, M. G. (2013). Revised status of Chloridea Duncan and (Westwood), 1841, for the Heliothis virescens species group (Lepidoptera: Noctuidae: Heliothinae) based on morphology and three genes. *Systematic Entomology*, *38*(3), 523-542. https://doi.org/10.1111/syen.12010

Reisenman, C. E., Dacks, A. M., & Hildebrand, J. G. (2011). Local interneuron diversity in the primary olfactory center of the moth Manduca sexta. *J Comp Physiol A Neuroethol Sens Neural Behav Physiol*, *197*(6), 653-665. https://doi.org/10.1007/s00359-011-0625-x

Robertson, H. M., & Wanner, K. W. (2006). The chemoreceptor superfamily in the honey bee, Apis mellifera: expansion of the odorant, but not gustatory, receptor family. *Genome Res*, *16*(11), 1395-1403. https://doi.org/10.1101/gr.5057506

Robertson, H. M., Warr, C. G., & Carlson, J. R. (2003). Molecular evolution of the insect chemoreceptor gene superfamily in Drosophila melanogaster. *Proc Natl Acad Sci U S A*, *100 Suppl 2*(suppl_2), 14537-14542. https://doi.org/10.1073/pnas.2335847100

Rostelien, T., Borg-Karlson, A. K., & Mustaparta, H. (2000). Selective receptor neurone responses to E-beta-ocimene, beta-myrcene, E,E-alpha-farnesene and homo-farnesene in the moth Heliothis virescens, identified by gas chromatography linked to electrophysiology. *Journal of Comparative Physiology A*, *186*(9), 833-847. https://doi.org/10.1007/s003590000136

Rostelien, T., Stranden, M., Borg-Karlson, A. K., & Mustaparta, H. (2005). Olfactory receptor neurons in two Heliothine moth species responding selectively to aliphatic green leaf volatiles, aromatic compounds, monoterpenes and sesquiterpenes of plant origin. *Chem Senses*, *30*(5), 443-461. https://doi.org/10.1093/chemse/bji039

Sane, S. P., Dieudonne, A., Willis, M. A., & Daniel, T. L. (2007). Antennal mechanosensors mediate flight control in moths. *Science*, *315*(5813), 863-866. https://doi.org/10.1126/science.1133598

Sato, K., Pellegrino, M., Nakagawa, T., Nakagawa, T., Vosshall, L. B., & Touhara, K. (2008). Insect olfactory receptors are heteromeric ligand-gated ion channels. *Nature*, *452*(7190), 1002-1006. https://doi.org/10.1038/nature06850

Schindelin, J., Arganda-Carreras, I., Frise, E., Kaynig, V., Longair, M., Pietzsch, T., Preibisch, S., Rueden, C., Saalfeld, S., Schmid, B., Tinevez, J. Y., White, D. J., Hartenstein, V., Eliceiri, K., Tomancak, P., & Cardona, A. (2012). Fiji: an open-source platform for biological-image analysis. *Nat Methods*, *9*(7), 676-682. https://doi.org/10.1038/nmeth.2019

Schneiderman, A. M., Matsumoto, S. G., & Hildebrand, J. G. (1982). Trans-sexually grafted antennae influence development of sexually dimorphic neurones in moth brain. *Nature*, *298*(5877), 844-846. https://doi.org/10.1038/298844a0

Seki, Y., & Kanzaki, R. (2008). Comprehensive morphological identification and GABA immunocytochemistry of antennal lobe local interneurons in Bombyx mori. *Journal of Comparative Neurology*, *506*(1), 93-107. https://doi.org/10.1002/cne.21528

Senatore, A., Reese, T. S., & Smith, C. L. (2017). Neuropeptidergic integration of behavior in Trichoplax adhaerens, an animal without synapses. *J Exp Biol*, *220*(Pt 18), 3381-3390. https://doi.org/10.1242/jeb.162396

Shields, V. D. C. (2004). Ultrastructure of Insect Sensilla. In *Encyclopedia of Entomology* (pp. 2408-2420). Springer Netherlands. https://doi.org/10.1007/0-306-48380-7_4455

Silbering, A. F., & Benton, R. (2010). Ionotropic and metabotropic mechanisms in chemoreception: 'chance or design'? *EMBO Rep*, *11*(3), 173-179. https://doi.org/10.1038/embor.2010.8

Stensaas, L. J., Lavker, R. M., Monti-Bloch, L., Grosser, B. I., & Berliner, D. L. (1991). Ultrastructure of the human vomeronasal organ. *J Steroid Biochem Mol Biol*, *39*(4B), 553-560. https://doi.org/10.1016/0960-0760(91)90252-z

Su, C. Y., Menuz, K., Reisert, J., & Carlson, J. R. (2012). Non-synaptic inhibition between grouped neurons in an olfactory circuit. *Nature*, *492*(7427), 66-71. https://doi.org/10.1038/nature11712

Suzuki, J., & Osumi, N. (2015). Neural crest and placode contributions to olfactory development. *Curr Top Dev Biol*, *111*, 351-374. https://doi.org/10.1016/bs.ctdb.2014.11.010

Tangtrakulwanich, K., Chen, H., Baxendale, F., Brewer, G., & Zhu, J. J. (2011). Characterization of olfactory sensilla of Stomoxys calcitrans and electrophysiological responses to odorant compounds associated with hosts and oviposition media. *Med Vet Entomol*, *25*(3), 327-336. https://doi.org/10.1111/j.1365-2915.2011.00946.x

Tay, W. T., Soria, M. F., Walsh, T., Thomazoni, D., Silvie, P., Behere, G. T., Anderson, C., & Downes, S. (2013). A brave new world for an old world pest: Helicoverpa armigera (Lepidoptera: Noctuidae) in Brazil. *PLoS One*, *8*(11), e80134. https://doi.org/10.1371/journal.pone.0080134

Vickers, N. J., & Baker, T. C. (1991). The Effects of Unilateral Antennectomy on the Flight Behavior of Male Heliothis-Virescens in a Pheromone Plume. *Physiological Entomology*, *16*(4), 497-506. https://doi.org/10.1111/j.1365-3032.1991.tb00589.x

Vosshall, L. B., & Hansson, B. S. (2011). A unified nomenclature system for the insect olfactory coreceptor. *Chem Senses*, *36*(6), 497-498. https://doi.org/10.1093/chemse/bjr022

Vosshall, L. B., Wong, A. M., & Axel, R. (2000). An olfactory sensory map in the fly brain. *Cell*, *102*(2), 147-159. https://doi.org/10.1016/s0092-8674(00)00021-0

Wang, H. L., Zhao, C. H., & Wang, C. Z. (2005). Comparative study of sex pheromone composition and biosynthesis in Helicoverpa armigera, H. assulta and their hybrid. *Insect Biochem Mol Biol*, *35*(6), 575-583. https://doi.org/10.1016/j.ibmb.2005.01.018

Wehr, M., & Laurent, G. (1996). Odour encoding by temporal sequences of firing in oscillating neural assemblies. *Nature*, *384*(6605), 162-166. https://doi.org/10.1038/384162a0

Wernecke, K. E., Vincenz, D., Storsberg, S., D'Hanis, W., Goldschmidt, J., & Fendt, M. (2015). Fox urine exposure induces avoidance behavior in rats and activates the amygdalar olfactory cortex. *Behav Brain Res*, *279*, 76-81. https://doi.org/10.1016/j.bbr.2014.11.020

Wicher, D. (2015). Chapter Two - Olfactory Signaling in Insects. In R. Glatz (Ed.), *Progress in Molecular Biology and Translational Science* (Vol. 130, pp. 37-54). Academic Press. https://doi.org/10.1016/bs.pmbts.2014.11.002

Wu, H., Xu, M., Hou, C., Huang, L. Q., Dong, J. F., & Wang, C. Z. (2015). Specific olfactory neurons and glomeruli are associated to differences in behavioral responses to pheromone components between two Helicoverpa species. *Front Behav Neurosci*, *9*(206), 206. https://doi.org/10.3389/fnbeh.2015.00206

Zhang, J., Walker, W. B., & Wang, G. (2015a). Chapter Five - Pheromone Reception in Moths: From Molecules to Behaviors. In R. Glatz (Ed.), *Progress in Molecular Biology and Translational Science* (Vol. 130, pp. 109-128). Academic Press. https://doi.org/10.1016/bs.pmbts.2014.11.005

Zhang, J., Wang, B., Dong, S., Cao, D., Dong, J., Walker, W. B., Liu, Y., & Wang, G. (2015b). Antennal transcriptome analysis and comparison of chemosensory gene families in two closely related noctuidae moths, Helicoverpa armigera and H. assulta. *PLoS One*, *10*(2), e0117054. https://doi.org/10.1371/journal.pone.0117054

Zhang, S., Maida, R., & Steinbrecht, R. A. (2001). Immunolocalization of odorant-binding proteins in noctuid moths (Insecta, Lepidoptera). *Chem Senses*, *26*(7), 885-896. https://doi.org/10.1093/chemse/26.7.885

Zhao, X. C., Chen, Q. Y., Guo, P., Xie, G. Y., Tang, Q. B., Guo, X. R., & Berg, B. G. (2016). Glomerular identification in the antennal lobe of the male moth Helicoverpa armigera. *Journal of Comparative Neurology*, *524*(15), 2993-3013. https://doi.org/10.1002/cne.24003

Appendix A

Confocal stack images, sample 17

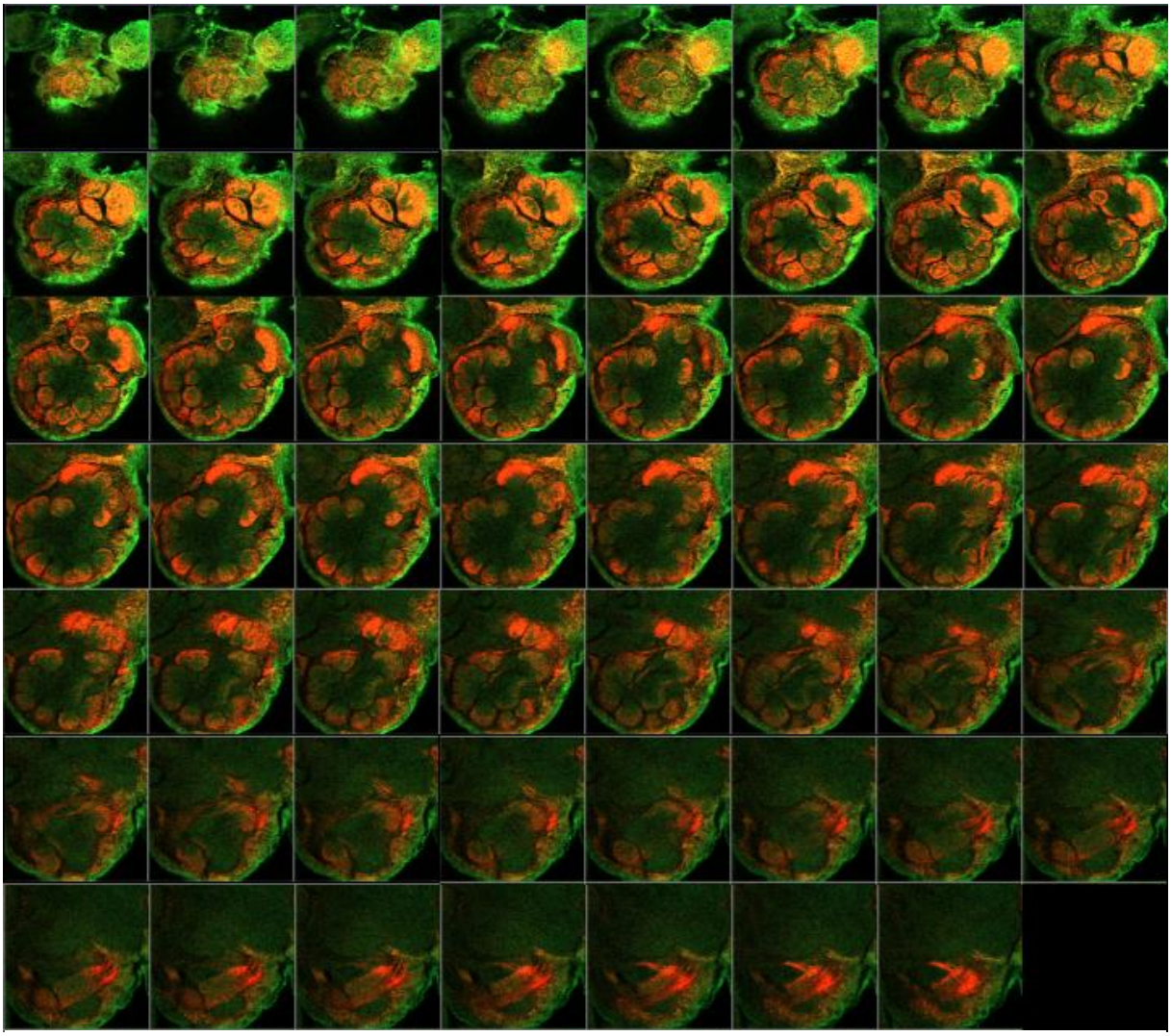

Figure A1. **Raw confocal data from proximal sample used for reconstruction.**

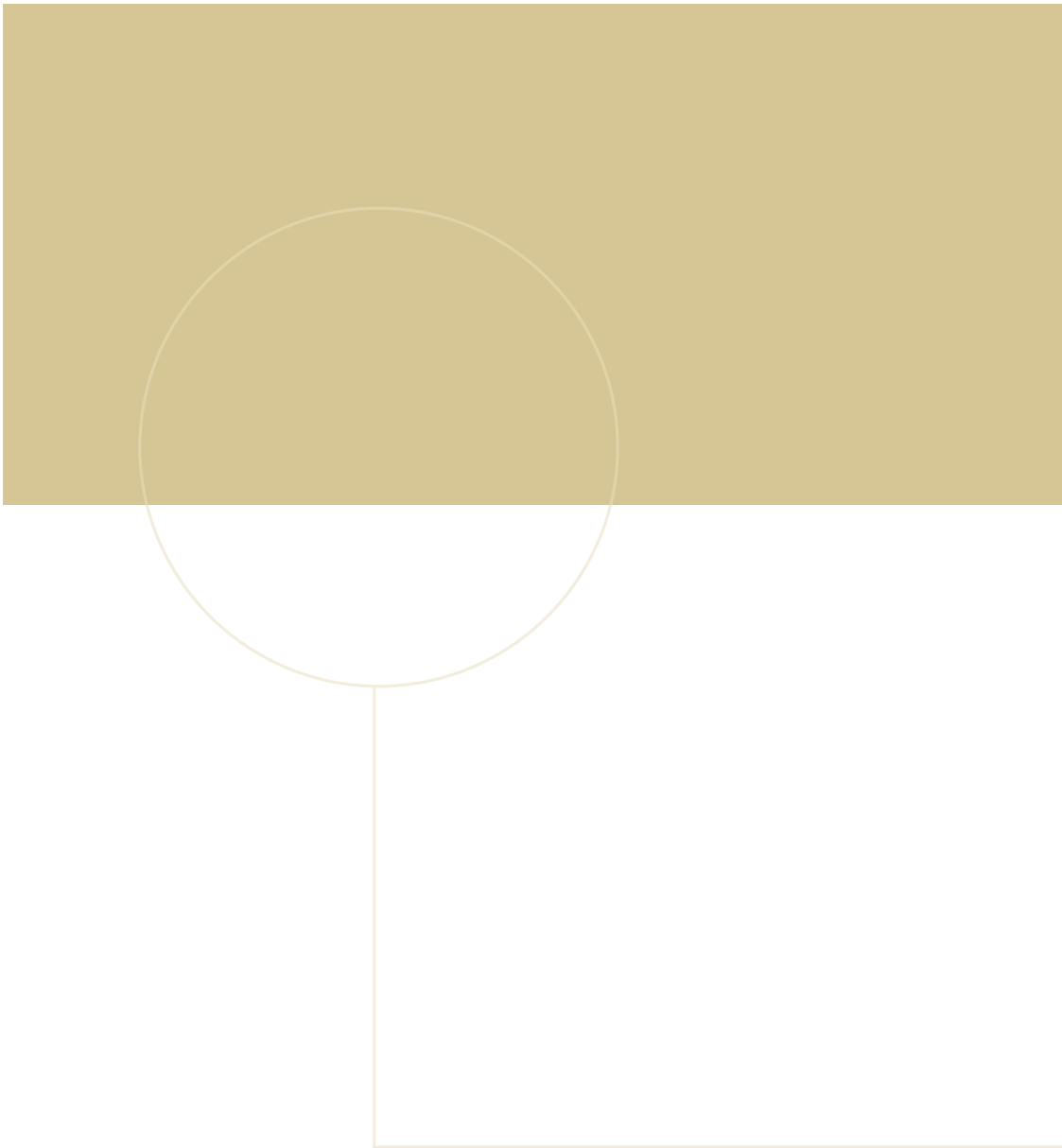

NTNU

Norwegian University of
Science and Technology